

# Regioselective Synthesis of Conformationally Designed Porphyrins with Mixed *meso*-Substituent Types and Distortion Modes

Mathias O. Senge\*<sup>[a]</sup> and Ines Bischoff<sup>[a]</sup>

**Keywords:** Conformation analysis / C–C coupling / Lithium / Porphyrinoids / Structure–activity relationships

Porphyrins can be substituted easily and in high yield at the *meso* positions by using organolithium reagents. When  $S_4$ -symmetric porphyrins such as 2,3,7,8,12,13,17,18-octaethylporphyrins are used as starting materials, it is possible to perform four such substitution reactions in sequence, resulting in the formation of nona-, deca-, undeca-, and dodecasubstituted porphyrins. Introduction of the first and second *meso* substituents can be achieved in almost quantitative yields, while the third and fourth *meso* substitutions proceed in about 50–70% yield with the remainder of the starting material being converted into stable porphomethenes. When one *meso* substituent is already present, introduction of the second residue proceeds with regiochemical preference for the 5,10-orientation over the 5,15-orientation, permitting a directed synthesis of 5,10-disubstituted porphyrins. Direct oxidation of the Meisenheimer-type intermediate formed after addition of RLi permits the introduction of two *meso* substituents in a one-pot reaction, again with preferential formation

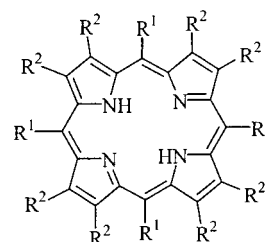
of the 5,10-disubstituted product. Using BuLi and PhLi as representative alkyl and aryllithium reagents, general reaction sequences were developed. These allow the preparation of *meso*-substituted octaethylporphyrins with almost any desired regiochemical combination of alkyl and aryl substituents. The synthesis of asymmetric, chiral, dodecasubstituted porphyrins can now be achieved in 4 to 6 steps, with overall yields in the range of 20–30%. X-ray crystallographic studies of the reaction products provided the means for the first analysis of the conformational effects of different types and arrangements of *meso* substituents present in one molecule. The results indicate that, depending on substituent type and localization, a mixing of distortion modes occurs. This offers significant opportunities for modulating the conformation, and thus the physicochemical properties, of these macrocycles and provides for the targeted design of biomimetic and potentially catalytically active porphyrins with specific conformations and binding cavities.

## Introduction

Conformationally designed biomimetic systems and the study of conformational control of biological reactions are becoming topics of active research at the interface of chemistry and biology.<sup>[1]</sup> In this context, the interrelationship between macrocycle conformation and physicochemical properties in porphyrins is emerging as a topic of special biological relevance. Various nonplanar conformations have been observed for the porphyrinoid cofactors involved in photosynthesis, electron transfer, and respiration, and it is now believed that the physicochemical properties of the natural tetrapyrroles are fine-tuned by means of steric interactions with the protein skeleton in a conformational control process.<sup>[1b,1c,2–5]</sup> Indeed, dynamic conformation changes and redox-dependent changes of the porphyrin conformation in proteins have now been confirmed.<sup>[4]</sup> Different macrocycle conformations have been described for all tetrapyrrole classes including porphyrins, hydroporphyrins, and corrins.<sup>[5]</sup>

In order to gain better insight into these processes and to establish conformational control firmly as one process for the regulation of macrocycle properties, a multitude of synthetic model compounds have been studied.<sup>[2]</sup> In par-

ticular, highly substituted porphyrins have been used prominently in this area.<sup>[2,6]</sup> Typical examples (Scheme 1) are the dodecasubstituted porphyrins **1–4** and 5,10,15,20-tetraalkylporphyrins (such as **5**).<sup>[10–12]</sup> These simple, symmetric porphyrins are easily accessible through pyrrole tetramerization reactions or by derivatization of **6**. All of the dodecasubstituted compounds display a highly nonplanar macrocyclic character, due to steric hindrance of the *meso* substituents with the flanking  $\beta$  substituents. To a first approximation, highly substituted porphyrins with  $C_m$ -sp<sup>2</sup> substituents (e.g. aryl) exhibit saddle shaped macrocyclic natures, while porphyrins with  $C_m$ -sp<sup>3</sup> substituents (e.g. alkyl groups) show *ruf* distortion.



- 1**  $R^1 = \text{Ph}, R^2 = \text{Et}$
- 2**  $R^1 = R^2 = \text{Ph}$
- 3**  $R^1 = \text{Bu}, R^2 = \text{Et}$
- 4**  $R^1 = \text{Ph}, R^2 = \text{Br}$
- 5**  $R^1 = t\text{Bu}, R^2 = \text{H}$
- 6**  $R^1 = \text{Ph}, R^2 = \text{H}$

Scheme 1

<sup>[a]</sup> Institut für Chemie, Organische Chemie, Freie Universität Berlin, Takustrasse 3, 14195 Berlin, Germany  
Fax: (internat.) +49 30 / 838 55163  
E-mail: mosenge@chemie.fu-berlin.de

Contrary to the situation with simple synthetic, symmetric porphyrins, natural tetrapyrrole chromophores have asymmetric substituent patterns and generally exhibit mixed distortion modes. The relative contribution of individual distortion modes (*ruf*, *sad*, *wav*, *dome*, etc.)<sup>[13]</sup> is characteristic for different functional classes of porphyrin-containing proteins.<sup>[14]</sup> Thus, asymmetrically substituted porphyrins with nonplanar macrocycles are needed to delineate the relative contributions and effects of individual substituents and their regiochemical arrangement on the functional properties. There have been only a few described examples of highly substituted porphyrins with different  $\beta$  or *meso* substituents,<sup>[15]</sup> or of porphyrins with incremental nonplanarity,<sup>[16]</sup> indicating that a substituent-induced mixing of distortion modes can occur.<sup>[17]</sup>

While synthetic strategies are available in principle for  $\beta$  substituent mixing, no rational synthesis of porphyrins with different regiochemical arrangements of *meso* substituents existed until recently.<sup>[12,18]</sup> One possible avenue involves the use of organolithium reagents for *meso* functionalization of tetrapyrroles.<sup>[9,19,20]</sup> The reaction between porphyrins and LiR is similar to the Ziegler alkylation,<sup>[21]</sup> and made *meso* substitution of porphyrins possible in excellent yields. Here we report that this reaction can be utilized for the synthesis of conformationally planned porphyrins with different types and numbers of *meso* substituents in a defined regiochemical arrangement and describe structural studies aimed at elucidating the conformational behavior of porphyrins with mixed distortion modes.

## Results and Discussion

### Syntheses

Initial studies have shown that it is possible, using four successive addition-oxidation cycles, to substitute all *meso* positions with BuLi.<sup>[9,19]</sup> This indicated that it should be possible to synthesize regiochemically pure porphyrins with different types and numbers of *meso* substituents, by choosing an appropriate sequence for the individual LiR reagents. As *meso* alkyl and *meso* aryl substituents flanked by  $\beta$  alkyl or aryl residues generally give rise to different distortion modes, we chose BuLi and PhLi as standard reagents with which test the feasibility of this approach. Octaethylporphyrin (**7**) and its nickel complex (**8**) were used as starting materials, as a large body of structural data for highly substituted porphyrins incorporating the octaethylporphyrin motif is available.<sup>[2,22]</sup>

Treatment of **8** with either BuLi or PhLi, followed by hydrolysis of the intermediate and oxidation of the porphodimethene with DDQ, yielded the respective mono-*meso*-substituted porphyrins **12** and **13**, respectively. Even when sterically more hindered nucleophiles such as *s*BuLi were used, the product **11** was obtained in good yield (82%, Figure 1). However, treatment with *t*BuLi or *i*PrLi and heating to 40 °C in the presence of base resulted only in recovery

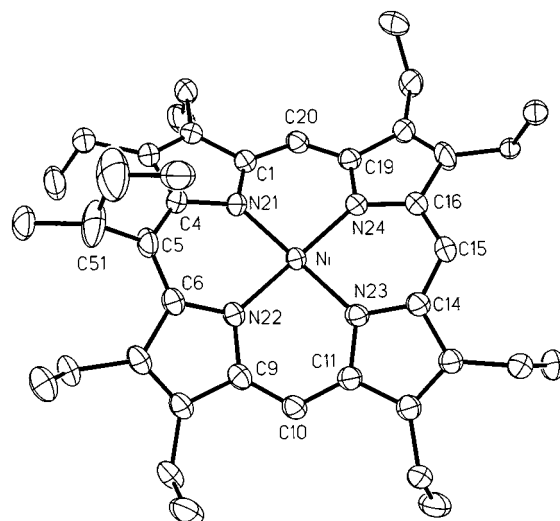
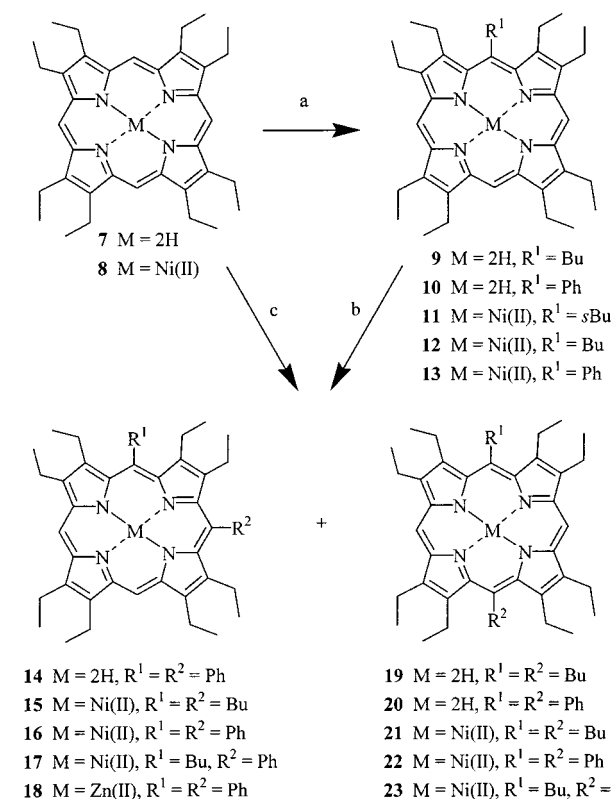


Figure 1. View of the molecular structure of **11** in the crystal. Thermal ellipsoids give 50% occupancy, hydrogen atoms and disordered positions have been omitted for clarity. Selected bond lengths: Ni–N21 1.908(3), Ni–N22 1.908(3), Ni–N23 1.913(3), Ni–N24 1.916(3) Å

of starting material and polar, blue-colored bands: – i.e., ring-opened products.

Compounds such as **9** and **10** were then used as starting materials for introduction of a second residue at a  $C_m$  position. Here, two products are possible: the 5,10- and 5,15-disubstituted regioisomers. Indeed, both isomers were formed (sequence of reactions a and b in Scheme 2), but with a general preference for the 5,10-product over the 5,15-regioisomer. Treatment of **10** with PhLi gave **14** and **20** in 84 and 4% yields, while treatment of **13** with BuLi gave **17** in 71 and **23** in 14% yields. The main benefit of this step lies in the convenient means of access now open to 5,10-disubstituted porphyrins. No rational method previously existed for the preparation of such compounds,<sup>[23]</sup> and even cross-condensations would require use of three different aldehydes and be likely to present an insurmountable chromatographic problem.

Surprisingly, simple variation of the reaction conditions used for the first substitution of **8** facilitated another easy means of access to 5,10-disubstituted porphyrins. When the oxidant DDQ was added to the reaction mixture immediately after addition of LiR – i.e., with omission of the hydrolysis step – two products were observed. With PhLi, these were identified as the monosubstituted product **13** (26%) and the disubstituted porphyrin **16** (12%). Thus, two residues had been introduced into the *meso* positions in one step (reaction c in Scheme 2). Similar products (**12** and **15** in 38% and 34% yield, respectively) were obtained from the reaction between **8** and BuLi. In addition, we observed the formation of two orange products, which were identified as porphodimethenes. Here, only the solvent or an intramolecular hydrogen exchange can be responsible for protonation of the intermediates. This observation for  $\beta$ -substituted porphyrins is in striking contrast to our results obtained with  $\beta$ -unsubstituted 5,15-diarylporphyrins. When these were treated with LiR/DDQ under similar conditions, a radical-

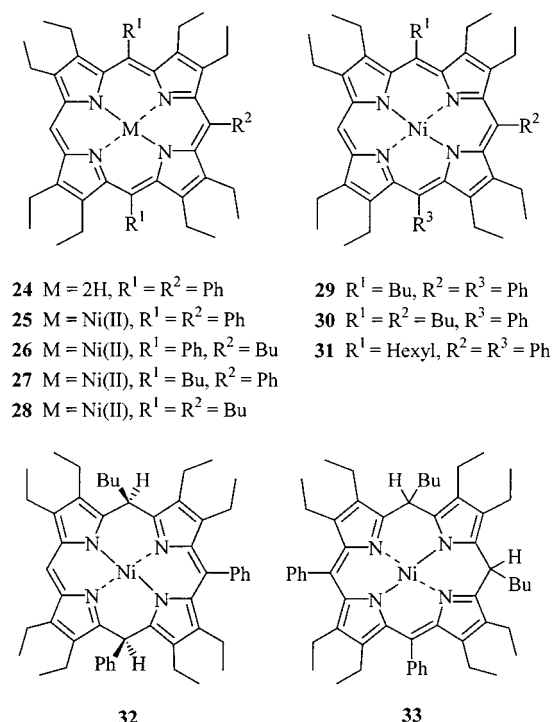


Scheme 2. a: R<sup>1</sup>Li, H<sub>2</sub>O, DDQ; b: R<sup>2</sup>Li, H<sub>2</sub>O, DDQ; c: R<sup>1</sup>Li/R<sup>2</sup>Li, DDQ

induced dimerization to *meso-meso*-linked bisporphyrins was observed.<sup>[19a]</sup> Such a pathway is obviously prohibited here for steric reasons.

Subsequent synthetic transformations were then concerned with the synthesis of 5,10,15-trisubstituted and 5,10,15,20-tetrasubstituted porphyrins (Scheme 3). It proved possible to introduce the third *meso* substituent into the porphyrin macrocycle in about 60–80% yield. For example, treatment of the free base **20** with PhLi gave the triphenylated porphyrin **24** in 70% yield, while treatment of the nickel(II) complex **22** with BuLi gave **26** in 60% yield.

However, a convenient means of access to ABC-porphyrins relies on the use of 5,10-disubstituted porphyrins (AB-type) as starting materials for reaction with organolithium compounds. Such a reaction can give two different regioisomers, which should be chiral. Firstly, we treated **16** with BuLi to give **29** in 57% yield, with the remainder of the starting material being converted into the porphodimethenes **32** and **33** (see below). Compound **17**, as expected, reacted with BuLi under formation of two different products. The main product, formed in 71% yield, was compound **27**, in which the new butyl group had been introduced at the *meso* position opposite to the butyl moiety already present in the molecule ('pseudo-para'). As there is a general preference for introduction of a novel *meso* substituent adjacent to one already present, this indicates that, in **17**, the aryl ring directs more strongly than the alkyl group does. The other isomer, **30**, was obtained in only 4.5% yield. In addition, a small amount of a mixture of porphodimethenes was formed. Treatment of 5,10-disubsti-

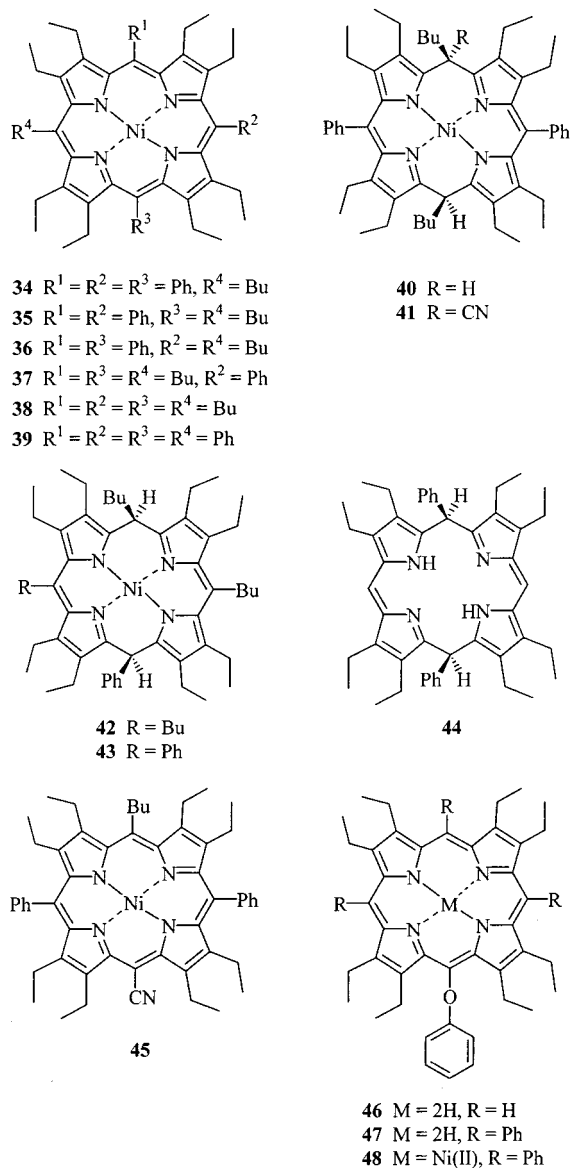


Scheme 3

tuted octaethylporphyrin free bases with ArLi generally resulted in recovery of the starting material, while treatment of 5,10-disubstituted octaethylporphyrin free bases with alkylolithium was not expected to be synthetically useful for the preparation of undecasubstituted porphyrins (low yields).

Successive introduction of further *meso* substituents into an octa-β-substituted porphyrin resulted in more distorted porphyrins, with a concomitant increase in the tendency to undergo side reactions or to form stable porphodimethenes (Scheme 4). Thus, introduction of a fourth *meso* substituent into a 5,10,15-tri-*meso*-substituted porphyrin generally proceeded with the lowest yields in this series: typically about 40–50% of the target porphyrin. For example, compound **25** was converted (with BuLi) into **34** in 47% yield, **30** in **35** in 48%, **26** in **36** in 51% and **27** into **37** in 54% yield.

In analogy to the reaction between **8** and RLi followed by direct oxidation without hydrolysis (path c in Scheme 2), we attempted a synthesis of dodecasubstituted, A<sub>2</sub>B<sub>2</sub>-type porphyrins in a two-step reaction from **8**. However, treatment of decasubstituted porphyrins with, for example, BuLi and direct oxidation with DDQ gave only minor quantities of the desired dodecasubstituted porphyrins (yield < 5%, detection only by TLC). For example, treatment of **16** with BuLi and direct oxidation gave **29** in 61% yield, accompanied by two hydroporphyrins. In the reaction sequence involving **16**, BuLi, H<sub>2</sub>O, and DDQ, the yield of **29** was similar (57%). However, at least three porphodimethenes were formed as side products. Similarly, treatment of **16** with hexyllithium, followed by hydrolysis and oxidation with DDQ, gave **31** in 62% yield (plus 2 hydroporphyrins), while the same procedure without the use of water gave the undecasubstituted porphyrin **31** in 60% yield as the main prod-



Scheme 4

uct. Omission of the hydrolysis step generally resulted in a more facile chromatographic workup, as formation of porphodimethenes was less and chromatographic purification easier.

As mentioned, brown products were often observed as side products in the trisubstitution or tetrasubstitution reactions. UV/Vis spectroscopy of the intensively red-colored fractions showed absorption bands typical of porphodimethenes (formally, 5,15- or 5,10-dihydroporphyrins). Thin layer chromatography of the side products indicated the formation of at least one such compound in these reactions and the separation and characterization of these products proved to be difficult. In several cases, however, at least one of these side products could be identified. For example, the synthesis of **29** was accompanied by the formation of **32**, the expected (intermediate) porphodimethene, and **33**, a doubly butylated product. The conversion of **26** into **36** was even more complex when the hydrolysis step was omitted

during the synthesis in an attempt to suppress porphodimethene formation. Nevertheless, the porphyrin **36**, the porphodimethene (**40**, in 19% yield) and a cyano derivative (**41**, in 23% yield) were isolated from the reaction mixture. The porphodimethene **42** was isolated in 14% yield as a side product from the synthesis of **37** by butylation of **27**. Preliminary spectroscopic data indicated that the analogous compound **43** was formed during the conversion of **29** to **35**.

The tendency towards the formation of these hydroporphyrins is directly related to the steric demand and the type of distortion in the starting material. Thus, the higher the degree of ruffling in the starting materials – i.e., the larger the number of *meso* alkyl substituents – the higher the propensity of these compounds to form stable hydroporphyrins. Obviously, the isolated hydroporphyrins are different from those porphomethenes and porphodimethenes that occur as intermediates on the pathway to the target porphyrins. This was confirmed by the stability of the isolated porphodimethenes towards oxidants such as DDQ or air. Compounds **32** and **33** could also be treated with *p*-chloranil or bromine and were found to be stable.<sup>[24]</sup> Quite possibly, the difference between the porphodimethenes functioning as intermediates in porphyrin formation and those isolated in stable (nonoxidizable) form is the configuration of the  $\text{sp}^3$ -hybridized centers. So far, all stable porphodimethenes isolated by us and unambiguously characterized by X-ray crystallography have exhibited a *syn* diaxial orientation of the two respective *meso* substituents and a roof-type (folded) macrocycle conformation.<sup>[9a,25]</sup> Such a conformation offers the largest relief of steric strain for the bulky *meso* substituents (especially for alkyl residues) and would also require significant movements of sterically hindered groups if oxidation should proceed. In some instances, such stable porphodimethenes can also be obtained from standard porphyrin syntheses. For example, when we prepared **20** by a standard [2+2] condensation,<sup>[26]</sup> we obtained the novel porphodimethene **44** as a side product (in 5% yield).

Another surprising result of these studies concerned the difference in reactivity of BuLi versus PhLi with 5,10-disubstituted or 5,10,15-trisubstituted porphyrins. It was not possible to insert an aryl substituent at the 15 position of the (2,3,7,8,12,13,17,18-octaethylporphyrinato)nickel(II) skeleton with a 5,10 substituent pattern. For example, neither compound **15** nor compound **16** would react with PhLi under the reaction conditions used in this study, and the starting material was recovered.

The overall strategy to produce dodecasubstituted porphyrins with *meso* aryl groups should start with arylation of free base octaethylporphyrin. This makes use of the higher yields obtained by treatment of the free base with PhLi (quantitative, compared to 50% on treatment of the  $\text{Ni}^{\text{II}}$  complex).<sup>[9a]</sup> In addition, the failure to phenylate a 2,3,5,7,8,10,12,13,17,18-decasubstituted porphyrin dictates prior introduction of the aryl group unless the synthetic goal is a 5,15-diaryl substituent pattern. Nevertheless, the method described here represents a convenient method for synthesis of various *meso*-substituted porphyrins. Success-



ive introduction of four *meso* substituents into the octaethylporphyrin skeleton requires only 4–6 synthetic steps. For example, synthesis of compound **35** was accomplished by means of the sequence **7** → **10** → **14** → **16** → **29** → **35**, with an overall yield of 22%, while the porphyrin **37** was prepared through the sequence **7** → **10** → **13** → **17** → **27** → **37** in 26% yield. As these yields should be representative for the use of various alkyl and/or aryllithium reagents, the synthesis, in excellent overall yields, of highly complex porphyrins with four different *meso* functionalities is now possible.

In two instances, additional side reactions were observed. These involved *meso* cyanation and *meso* phenoxylation reactions. As described above, highly hindered porphyrins have a tendency to form stable porphodimethenes as substitution reaction side products. In order to circumvent this problem, we attempted to prevent the porphodimethene formation in the reaction between **22** and BuLi, giving **26**, by omitting the hydrolysis step. This resulted in the isolation of a 32% yield of the target porphyrin **26**, starting material, about a 15% yield of an uncharacterized mixture of porphodimethenes, and a 23% yield of a *meso* cyano-substituted heteroaromatic macrocycle (**45**). The presence of the cyano group was indicated by the respective IR ( $\nu_{\text{CN}} = 2204 \text{ cm}^{-1}$ ) and  $^1\text{H}$ ,C-COSY data (e.g., a weak, uncorrelated signal at  $\delta = 142.41$ ) and fully confirmed by a single-crystal X-ray structural analysis (Figure 2). Under standard reaction conditions (LiR,  $\text{H}_2\text{O}$ , DDQ), formation of this product was not observed. Reactions between porphyrins and cyanide are not unknown: for example, the oxidation of metalloporphyrins to  $\pi$  cations and subsequent reaction with nucleophiles such as  $\text{CN}^-$  is possible.<sup>[27]</sup> Similarly, an anodic electrochemical oxidation of a porphyrin followed by reaction with DDQ to form a *meso* cyano compound has been described.<sup>[28]</sup> In the case at hand, oxidation of the porphyrin was mediated by DDQ, which also served as source of the cyanide nucleophile for reaction with the  $\pi$  cation radical. An explanation for this reactivity can be provided by an examination of the redox chemistry of highly substituted porphyrins. Generally, a higher degree of nonplanarity (destabilization of the  $\pi$  system) in the compounds discussed here results in a lower oxidation potential. For example, the unhindered system **8** has an  $E_{1/2\text{ox}}$  of 1.15 V, (5,10,15,20-tetrabutylporphyrinato)nickel(II) an  $E_{1/2\text{ox}}$  of 0.93 V, while the highly hindered **38** exhibits an  $E_{1/2\text{ox}}$  of 0.56 V.<sup>[9b]</sup> Compound **26** should have an oxidation potential slightly higher than this. Thus, DDQ ( $E_{1/2\text{red}} = 0.51 \text{ V}$ ,  $E_{1/2\text{ox}} = 0.75 \text{ V}$ )<sup>[29]</sup> should easily generate the cation radical.

A different side product was observed when the employed stock solutions of PhLi had been exposed for some time to air and humidity. Use of PhLi in the reaction with **7** resulted in the formation of a polar side product in 17 to 25% yield, depending on the age of the stock solutions. This compound was identified as the *meso* phenoxyated product **46**. A similar product, **47**, was obtained from **24**. After metallation with nickel(II) acetate, the presence of the *meso* phenoxy group was unambiguously confirmed by X-ray

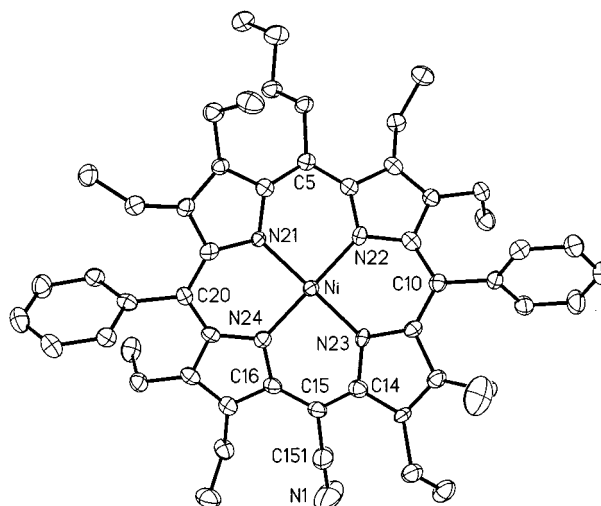


Figure 2. View of the molecular structure of **45** in the crystal. Thermal ellipsoids give 50% occupancy, hydrogen atoms have been omitted for clarity. Selected bond lengths and angles: Ni–N21 1.924(3), Ni–N22 1.909(3), Ni–N23 1.912(3), Ni–N24 1.908(3), C15–C151 1.427(7), C151–N1 1.159(7) Å, C14–C15–C151 117.0(4), C16–C15–C151 118.8(4), C15–C151–N1 177.4(8)°

crystallography on the  $\text{Ni}^{\text{II}}$  complex **48** (Figure 3). Attempts to perform a radical-induced synthesis of such compounds by treating either the free base **7** or the nickel(II) complex **8** with basic solutions of phenolate in the presence of  $\text{H}_2\text{O}_2$ , followed by oxidation with DDQ, have so far resulted only in recovery of the starting material; further experiments are in progress. To the best of our knowledge, direct phenoxylation of porphyrins has been described only at the 2-position, as the product of the reaction between (2-nitro-5,10,15,20-tetraphenylporphyrinato)nickel(II) and phenol in DMF.<sup>[30]</sup> Steric effects appear to play a major role in this reaction; when  $\beta$ -unsubstituted 5,15-diphenylporphyrins were treated under the same conditions, only the formation of the 5,10,15-triphenyl derivative was observed.

### Structural Studies

The preparation of various macrocycles with mixed alkyl and aryl *meso* substituents successfully having been accomplished, it was necessary to investigate the macrocycle conformation of the target molecules in more detail. A first approximation for the overall degree of ring distortion may be inferred by comparison of the electronic absorption spectra with those of appropriate reference compounds. It is now established that one of the most obvious results of steric overcrowding at the periphery of heteroaromatic macrocycles, and thus nonplanarity, is a concomitant bathochromic shift of the absorption bands.<sup>[1b,9b,31]</sup> Table 1 lists the main Soret and long wavelength Q absorption maxima of several porphyrins. The results clearly show that successive introduction of peripheral substituents results in red shifting of the absorption bands. For example, the free bases **7**, **10**, **20**, **14**, **24**, and **1** constitute a series of macrocycles with increasing numbers of *meso* phenyl groups and exhibit long wavelength Q absorption bands at 620, 622, 627, 637, 635, and 686 nm, respectively.

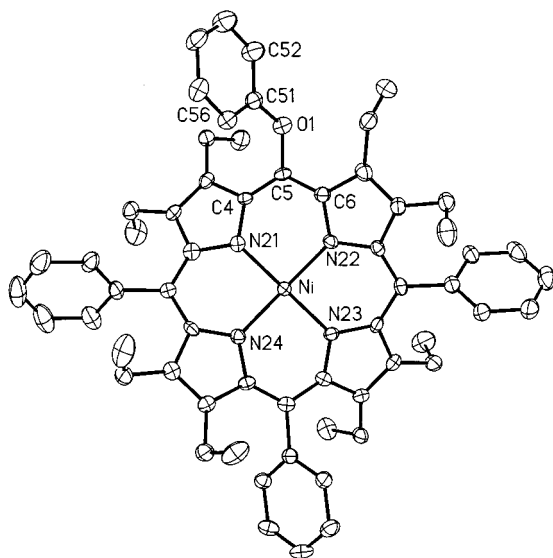


Figure 3. View of the molecular structure of **48** in the crystal. Thermal ellipsoids give 50% occupancy, hydrogen atoms have been omitted for clarity. Selected bond lengths and angles: Ni–N21 1.904(4), Ni–N22 1.909(4), Ni–N23 1.910(4), Ni–N24 1.925(4), C5–O1 1.400(6), O1–C51 1.382(6) Å, C4–C5–O1 118.8(4), C5–C6–O1 116.8(4), C5–O1–C51 117.4(4), O1–C51–C56 124.9(5), O1–C51–C52 114.7(5)°

Table 1. Soret and long wavelength Q-band absorption maxima of selected porphyrins in dichloromethane

Compound	<i>meso</i> substituent				$\lambda_{\text{max}}$ [nm]		ref.[a]	
	C5	C10	C15	C20				
free bases								
<b>7</b>	H	H	H	H	397	620	—	
<b>10</b>	Ph	H	H	H	404	622	[9a]	
<b>46</b>	OPh	H	H	H	405	625	t.w.	
<b>20</b>	Ph	H	Ph	H	410	627	[26]	
<b>14</b>	Ph	Ph	H	H	448	637	t.w.	
<b>24</b>	Ph	Ph	Ph	H	450	635	t.w.	
<b>1</b>	Ph	Ph	Ph	Ph	446	686	[7e]	
<b>47</b>	OPh	Ph	Ph	Ph	446	629	t.w.	
nickel(II) complexes								
<b>8</b>	H	H	H	H	391	551	—	
<b>13</b>	Ph	H	H	H	401	558	[9a]	
<b>22</b>	Ph	H	Ph	H	407	563	—	
<b>16</b>	Ph	Ph	H	H	412	568	t.w.	
<b>25</b>	Ph	Ph	Ph	H	418	579	t.w.	
<b>39</b>	Ph	Ph	Ph	Ph	432	585	[7g]	
<b>12</b>	Bu	H	H	H	410	572	[9a]	
<b>11</b>	<i>s</i> Bu	H	H	H	412	573	t.w.	
<b>21</b>	Bu	H	Bu	H	423	595	[9a]	
<b>15</b>	Bu	Bu	H	H	427	595	[9a]	
<b>28</b>	Bu	Bu	Bu	H	442	612sh	[9a]	
<b>38</b>	Bu	Bu	Bu	Bu	459	634	[9a,9b]	
<b>17</b>	Bu	Ph	H	H	418	582	t.w.	
<b>23</b>	Bu	H	Ph	H	418	572	t.w.	
<b>26</b>	Bu	Ph	H	Ph	423	579	t.w.	
<b>27</b>	Bu	Ph	Bu	H	432	607	t.w.	
<b>29</b>	Bu	Ph	Ph	H	426	590	t.w.	
<b>31</b>	Hexyl	Ph	Ph	H	426	590	t.w.	
<b>30</b>		Bu	Bu	Ph	H	434	606	t.w.
<b>34</b>		Bu	Ph	Ph	Ph	435	595	t.w.
<b>35</b>		Bu	Bu	Ph	Ph	438	601	t.w.
<b>36</b>		Bu	Ph	Bu	Ph	438	617	t.w.
<b>37</b>		Bu	Bu	Bu	Ph	450	627	t.w.
<b>45</b>		Bu	CN	Ph	Ph	436	633	t.w.
<b>48</b>		OPh	Ph	Ph	Ph	448	637	t.w.

<sup>[a]</sup> t.w.: this work.

In line with earlier results on *meso*-tetraphenylporphyrins with various numbers of  $\beta$ -ethyl substituents,<sup>[16b]</sup> siting of steric overcrowding in neighboring pyrrole quadrants (5,10) gives rise to absorption maxima at wavelengths longer (e.g. **14** = 448 and 637 nm) than those observed in porphyrins with steric hindrance imposed at opposite quadrants (5,15, e.g. **20** = 410 and 627 nm). An inspection of the metalloporphyrin absorption spectra shows similar trends. *Meso* alkyl substituents generally result in larger bathochromic shifts compared to *meso* aryl substituents. While absorption spectra can give an overall indication for the degree of non-planarity in solution, a more detailed analysis requires single-crystal X-ray crystallographic structure determinations and conformational analyses. Selected conformational and structural data for the nine compounds suitable for crystallographic investigation are compiled in Table 2.

The multitude of structural data available for so-called highly substituted porphyrins have enabled several general structural and conformational trends occurring upon porphyrin macrocycle distortion to be identified.<sup>[2]</sup> For example, compound **11** (Figure 1) bears a bulky *s*Bu substituent in a *meso* position. This results in an overall ruffled macrocycle, ruffling here being the result both of the small Ni ion with its concomitant Ni–N bond shortening<sup>[32]</sup> and of the steric hindrance arising from the *meso* substituent. The latter results in a significantly larger displacement of the substituted C<sub>m</sub> position (5) from the mean plane (0.87 Å), as compared to the unsubstituted positions (0.58–0.64 Å, see Table 2). Structurally, the most significant result is a smaller C<sub>a</sub>–C<sub>m</sub>–C<sub>a</sub> angle at this position [119.0(3)°] than that at the others or in the unsubstituted references compound **8** (124–125°).<sup>[33]</sup> In fact, this value is similar to the one found for the highly ruffled **38** [119.2(3)°].<sup>[9b]</sup> Thus, the presence of one very bulky group can result locally in distortions similar to those otherwise observed only in porphyrins with a larger number of steric interactions. Other general trends observed upon substituent-induced macrocycle distortion and mirrored here include metal-nitrogen bond shortening and C<sub>a</sub>–C<sub>m</sub> bond elongation. For a comparative discussion of these general effects, see the treatise by Senge.<sup>[2]</sup>

The structure of the free base **14** with two *meso* phenyl substituents at the 5 and 10 positions presents an interesting test case for the influence of the regiochemical orientation of the *meso* substituents on the conformation. The geometrical parameters for substituted and unsubstituted quadrants follow the general trends of highly substituted porphyrins. For example, the C<sub>a</sub>–C<sub>m</sub>–C<sub>a</sub> angles for C5 and C10 are 125.1(5)° and 125.5(4)°, respectively while those for the C15 and C20 positions are 127.5(4)° and 126.9(4)°. In octaethylporphyrin **7**, the average value for these positions is 127.6(1)°,<sup>[34]</sup> while in the highly substituted porphyrin **1** the average C<sub>a</sub>–C<sub>m</sub>–C<sub>a</sub> angle is 123.8°.<sup>[35]</sup> In contrast, the only 5,15-diphenyl structure available for comparison is that of 10,20-etioporphyrin II (2,8,12,18-tetraethyl-3,7,13,17-tetramethyl-5,15-diphenylporphyrin).<sup>[17]</sup> For this compound we found even larger differences between the substituted [123.8(2)°] and unsubstituted [131.7(3)°] C<sub>a</sub>–C<sub>m</sub>–C<sub>a</sub>

Table 2. Selected conformational parameters for the porphyrins studied and important reference compounds. Numbers are given relative to the least-squares plane for the four nitrogen atoms. Numbers listed for individual quadrants give the average values of geometrically equivalent positions in each quadrant

Compound	$\Delta 24^{[a]}$	$C_m$ -displacements [ $\text{\AA}$ ]					$C_b$ -displacements [ $\text{\AA}$ ] Quadrant					Pyrrole tilt [deg] Quadrant				
		average	C5	C10	C15	C20	average	N21	N22	N23	N24	average	N21	N22	N23	N24
free bases																
7 <sup>[34]</sup>	0.02	0.04					0.08					2.2				
10 <sup>[b]</sup> <sup>[9a]</sup>	0.04	0.07	0.10	0.08	0.07	0.03	0.08	0.08	0.09	0.09	0.06	2.6	3.2	2.1	3.0	2.2
DiPh-ETIO-II <sup>[c]</sup> <sup>[17]</sup>	0.03	0.10	0.11	*	*	0.08	0.12	0.12	*	*	0.11	3.5	4.3	*	*	2.6
14	0.39	0.1	0.12	0.10	0.06	0.11	0.76	0.78	1.20	0.72	0.34	20.8	18.9	30.3	17.3	16.6
24	0.523	0.15	0.1	0.1	0.34	0.05	1.05	0.96	1.25	1.42	0.57	27.8	24.4	34.0	38.3	14.3
1 <sup>[35]</sup>	0.54	0.03					1.17					31.2				
nickel(II) complexes																
8 tricl. <sup>[33a]</sup>	0.02	0.03					0.06					1.7				
8 tetra. <sup>[33b]</sup>	0.26	0.51					0.27					16.4				
13 <sup>[9a]</sup>	0.26	0.52	0.51	0.52	0.54	0.49	0.22	0.23	0.21	0.24	0.20	16.8	15.5	15.6	19.3	16.9
12 <sup>[9a]</sup>	0.34	0.69	0.89	0.64	0.58	0.66	0.27	0.32	0.29	0.22	0.23	21.9	26.3	23.3	18.0	19.8
11	0.335	0.69	0.87	0.66	0.58	0.64	0.26	0.28	0.29	0.23	0.24	27.7	19.3	26.7	38.9	25.7
16	0.476	0.27	0.31	0.23	0.26	0.28	0.84	0.83	1.03	0.82	0.69	20.6	19.5	25.4	20.6	16.7
23	0.343	0.69	0.76	0.70	0.61	0.69	0.27	0.27	0.25	0.28	0.28	21.8	22.1	21.1	22.2	21.7
26 <sup>[d]</sup>	0.491	0.65	0.75	0.59	0.58	0.66	0.72	0.79	0.83	0.57	0.68	25.6	29.1	29.0	17.4	26.7
	0.488	0.63	0.77	0.57	0.55	0.63	0.73	0.83	0.8	0.52	0.76	25.9	29.4	26.9	19.8	27.6
21 <sup>[b]</sup> <sup>[9a]</sup>	0.39	0.81	0.83	0.77	0.83	0.79	0.31	0.29	0.30	0.30	0.33	24.8	23.2	23.4	24.9	27.5
tricl. 15 <sup>[9a]</sup>	0.40	0.76	0.84	0.87	0.65	0.67	0.37	0.29	0.56	0.35	0.29	24.7	25.5	29.5	21.9	21.9
28 <sup>[9a]</sup>	0.45	0.93	0.94	1.04	0.94	0.81	0.34	0.33	0.35	0.37	0.32	28.7	28.0	29.1	30.9	26.9
38 <sup>[9b]</sup>	0.46	1.05					0.37					31.2				
39 <sup>[7g]</sup>	0.62	0.03					1.24					29.4				
48	0.597	0.04	0.01	0.03	0.03	0.08	1.19	1.11	1.15	1.25	1.25	27.6	25.3	26.4	29.2	29.6
45	0.594	0.34	0.26	0.31	0.37	0.40	1.07	1.22	1.15	0.99	0.91	26.8	30.3	28.6	25.6	22.8

<sup>[a]</sup>  $\Delta 24$  = average deviation of the 24 macrocycle atoms from their least-squares plane. – <sup>[b]</sup> Data for one of two crystallographically independent molecules. – <sup>[c]</sup> DiPh-ETIO-II = 2,8,12,18-tetraethyl-3,7,13,17-tetramethyl-5,15-diphenylporphyrin. – <sup>[d]</sup> Two crystallographically independent molecules.

angles. For 5,15-diaryl-2,3,7,8,12,13,17,18-octaalkylporphyrins, in-plane distortion – i.e., a rectangular distortion of the porphyrin macrocycle compound with concomitant widening of the  $C_a-C_m-C_a$  angles along the axis of the substituted *meso* positions – was found. This was evidenced by a very small  $\Delta 24$  value<sup>[36]</sup> of 0.04 Å, a maximum  $C_b$  displacement of 0.16 Å, and a significant core elongation ( $\Xi = -0.432$  Å).<sup>[17]</sup> In comparison, the structure of the 5,10-derivative **14** reported here featured a  $\Delta 24$  of 0.39 Å, a core size of 2.052 Å, and a  $\Xi$  of  $-0.048$  Å. The conformation of **14** (see Figure 7) is characterized by an asymmetric saddle distortion, with  $C_b$  displacements ranging from 0.34 to 1.2 Å and phenyl tilt angles of 53.9° and 53.7° for C5 and C10, respectively. Thus, just by going from the symmetric 5,15-diaryl pattern to a 5,10 pattern, the type of distortion is switched from in-plane to out-of-plane distortion. While the arrangement of the molecules of **14** in the crystal is unexceptional, this structure presents another intriguing example of the possibilities of appropriately use of functionalized nonplanar macrocycles for recognition and binding of small molecules. As shown in Figure 4, a dichloromethane of solvation is bound in one of the cavities formed by the nonplanar macrocycle.<sup>[37]</sup> In fact, besides a case of true hydrogen bonding involving **2**,<sup>[8c]</sup> this is only the second case in which it has been possible to show a direct interaction between a solvate molecule and the pyrrole nitrogen atoms. Here, the two solvate hydrogen atoms have close contacts with the N atoms (N22–H1S1 2.565 Å and N24–H1S2 2.540 Å).

The structure of **16** (not shown) shows typical structural parameters for a nonplanar porphyrin with significant degree of macrocycle distortion. The conformation is characterized by a mixture of *sad* and *ruf* distortions. The differences between substituted and unsubstituted *meso* quadrants are much less in the nickel derivative than in the free base or zinc(II) complex (see Figure 7). Noteworthy structural features are: relatively moderate phenyl tilt angles (60.5° and 75.5° for C5 and C10, respectively), a significant distortion of the 4N core with an alternating displacement of the nitrogen atoms by 0.16 Å from their least-squares plane, and significant differences in the bond lengths and angles involving substituted and unsubstituted *meso* positions.

The corresponding 5,10-dibutyl derivative **15** features almost purely ruffled conformations.<sup>[9a]</sup> Thus, the observation that, in dodecasubstituted porphyrins, *meso* alkyl substituents result in ruffling while *meso* aryl groups tend to promote saddle distortion, also applies to nickel porphyrins with an intermediate degree of “steric overload”. The overall degree of distortion ( $\Delta 24 = 0.48$  Å) is larger than that in some nonplanar dodecasubstituted porphyrins (for example, **38**,  $\Delta 24 = 0.46$  Å).<sup>[9b]</sup> This is a result of the contribution of both *ruf* and *sad* distortion, the latter producing larger  $\Delta 24$  values. Thus, for compounds with mixed distortion modes it is necessary to use separate descriptors for the saddle distortion (for example: pyrrole tilts or  $C_b$  displacements) and the ruffling (for example:  $C_m$  displacements or appropriate torsion angles) to describe the degree of con-

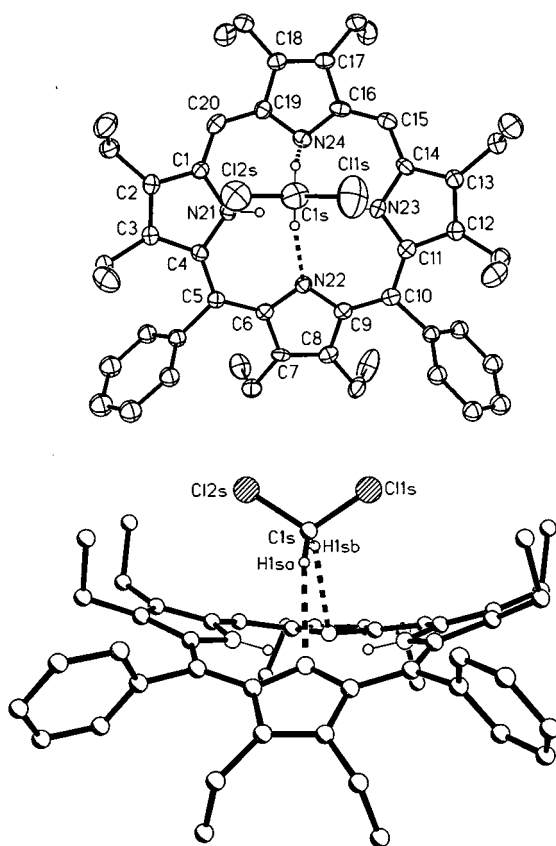


Figure 4. Top and side view of **14** with the loosely bound dichloromethane of solvation. Thermal ellipsoids are drawn for 50% occupancy, only selected hydrogen atoms shown. Selected bond lengths and angles: H1Sa–N22 2.565, H1Sb–N24 2.540 Å; C4–C5–C6 125.1(5), C9–C10–C11 125.5(4), C14–C15–C16 127.5(4), C19–C20–C1 126.9(4)°

formational distortion accurately. Similarly to that of the free base, the crystal structure of **16** contains a solvate molecule bound in the cavity formed by the macrocycle and the  $\beta$ -ethyl side chains.

For comparative structural analysis, the related zinc(II) complex **18** was prepared by metallation of **14**. Its crystal structure (not shown) shows that this compound had crystallized as a five-coordinated species, with a methanol bound as an axial ligand. The structural parameters of the core are similar to those of other five-coordinate zinc(II) porphyrins when an intermediate degree of macrocycle distortion is taken into account.<sup>[2,13]</sup> Selected bond lengths and angles are: Zn–N21 2.051(2), Zn–N22 2.071(2), Zn–N23 2.053(2), Zn–N24 2.043(2), Zn–O1A 2.236(2) Å; C4–C5–C6 125.9(3), C9–C10–C11 124.9(3), C14–C15–C16 126.9(3), C19–C20–C1 127.8(3)°. The central zinc(II) atom is displaced by 0.22 Å from the 4N plane. The macrocycle conformation is asymmetric, with a large saddle contribution, and shows its largest deviations from planarity for the C5 and C10 quadrants. At first glance, the overall conformation looks rather similar to that of the free base **14** (see Figure 7). However, **18**(MeOH) exhibits a small, but significant degree of ruffling. For comparison, the related zinc(II) complex of **1**, with an axial

methanol, represents a purely saddle distorted macrocycle, with  $C_b$  displacements of 1.09 Å.<sup>[7c]</sup>

The structure of the free base **25** with three *meso* phenyl groups (Figure 5) continues the trends seen in the structure of **14**. Again, the  $C_a$ – $C_m$ – $C_a$  angles are significantly smaller for the substituted *meso* positions [123.1(3), 123.0(3), and 123.6(3)° for C5, C10, C15] as compared to that in C20 [127.2(3)°]. Similar trends are observed in other geometrical parameters. For example, the average  $C_a$ – $C_m$  bond length of the substituted *meso* positions is 1.412(4) Å, compared to 1.391(4) Å for C20, and the N– $C_a$ – $C_b$  angles are smaller than those at C20 by 1° in the substituted quadrants, while the  $C_m$ – $C_a$ – $C_b$  angles are larger by about 3°. The overall conformation (see Figure 7) represents an asymmetric saddle distortion, with smaller  $C_b$  displacements for the hindered quadrants (average 0.96 to 1.42 Å, Table 2), compared to the C20 quadrant (0.57 Å). As indicated by the  $C_b$ – $C_b$  tilts in Figure 7, the asymmetric substitution of the *meso* quadrants results in a small but significant degree of ruffling. The core size is typical, at 2.052 Å, while the core elongation is relatively small at 0.111 Å.

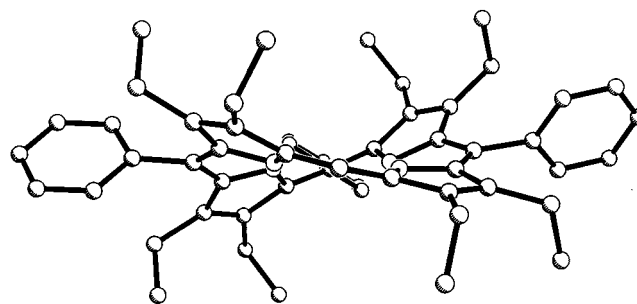


Figure 5. Side view of the molecular structure of **24** in the crystal. Hydrogen atoms have been omitted for clarity

Taking together the data for **7**,<sup>[34]</sup> **10**,<sup>[9a]</sup> **14**, 10,20-diphenyletioporphyrin<sup>[17]</sup> as a model for **20**, **24**, and **1**,<sup>[35]</sup> we now have a series of octaethylporphyrins with an incremental degree of *meso* substitution and nonplanarity. This series complements the series of tetraphenylporphyrins with incremental degrees of  $\beta$ -ethyl substitution that we described previously.<sup>[16b]</sup> Overall, both series exhibit similar trends in conformation changes, indicating that the way in which the degree of steric interactions is raised (either by *meso* arylation or  $\beta$ -alkylation) is irrelevant for *meso*-aryl  $\beta$ -alkyl porphyrins. Closer examination shows that in the intermediate cases, asymmetry of the *meso* arylation pattern results in a larger contribution of ruffling to the overall conformation.

We next studied two porphyrins with mixed *meso* substituent types and intermediate degrees of macrocycle distortion. The structure of **23** (not shown) represents an almost purely ruffled macrocycle conformation (see Figure 7). As expected, the *meso* displacement is slightly greater for the  $sp^3$  substituent at C5 (0.76 Å) than for the *meso*  $sp^2$  substituent ( $\delta C15$  = 0.61 Å). Structural differences between the individual quadrants (*meso*-H, *meso*-aryl, and *meso*-alkyl) agree well with those of the reference compounds containing only one type of substituents. More surprising is a comparison of the conformation with closely related molec-



ules. The nickel(II) complex **21**, with two 5,15 butyl groups, shows almost pure ruffling,<sup>[9a]</sup> while the nickel(II) chelate of 10,20-diphenyletioporphyrin represents a saddle distortion with a minor wave contribution.<sup>[17]</sup> Thus, in **23**, in which both one phenyl (phenyl tilt angle 87.3°) and one butyl group are present, the latter, with its tendency to induce ruffling, dominates the overall distortion mode of the macrocycle.

The structure of **26** gives even more evidence for the influence of the substituent type and pattern on the conformation (Figure 6). This compound crystallized with two independent molecules in the noncentrosymmetric space group  $P2_1$ . Because of the presence of three different types of *meso* substituents (H, Bu, and 2Ph) and the asymmetric macrocycle distortion, the molecule has two enantiotopic faces and is chiral. The overall conformation is characterized by both saddle distortion and ruffling (Figure 7). Again, the presence of one *meso* alkyl residue is sufficient to induce a significant degree of ruffling in the macrocycle. Note that the relative contribution of the individual distortion modes is strongly influenced by the exact type of the individual substituents. For example, (10,20-diphenyl-etioporphyrinato)nickel(II) substituted with either a 15-acrolein or a 15-formyl residue showed significant differences in the out-of-plane displacements and a reversal of the relative contributions from *ruf* and *sad* distortion modes.<sup>[17]</sup>

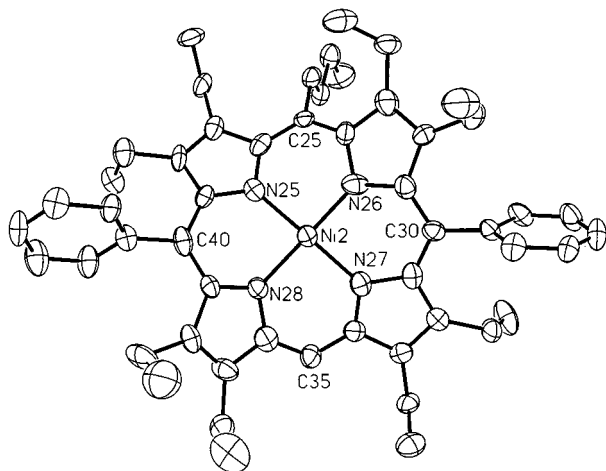


Figure 6. Top view of the molecular structure of one of the two crystallographically independent molecules of **26** in the crystal. Thermal ellipsoids are drawn for 50% occupancy; hydrogen atoms have been omitted for clarity. Selected bond lengths: molecule 1: Ni–N21 1.908(9), Ni–N22 1.920(9), Ni–N23 1.888(8), Ni–N24 1.918(8) Å; molecule 2: Ni–N25 1.897(8), Ni–N26 1.872(9), Ni–N27 1.932(9), Ni–N28 1.923(9) Å

So far, we have been able to characterize only two dodecasubstituted porphyrins with different *meso* substituents. The structure of **48** (Figure 3) represents a purely saddle distorted macrocycle conformation. Structural and conformational descriptors are very similar to those of the symmetric **39**.<sup>[7g]</sup> Surprisingly, the presence of the C5–O–Ph substituent exerts no significant influence on the conformation, as compared to **39**. Nevertheless, some differences are seen in the relevant bond lengths and angles. For example,

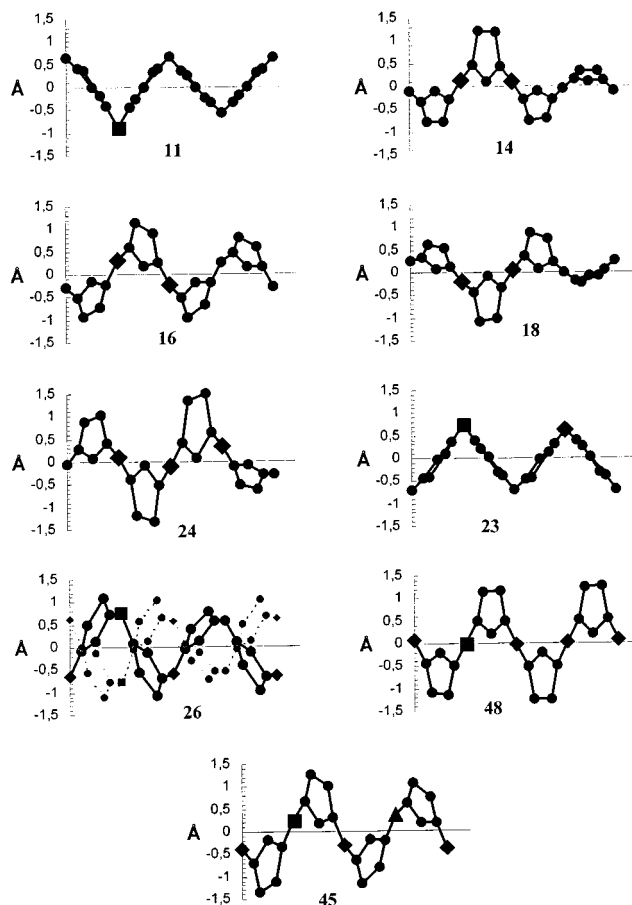


Figure 7. Skeletal deviation plots for selected nonplanar porphyrins. The x-axis is not to scale and the sequence of pyrrole rings follows the IUPAC nomenclature from left to right (N21, N22, N23, N24); ■ denotes a *meso*  $sp^3$  substituent, ◆ a *meso*  $sp^2$  substituent, and ▲ a *meso*  $sp$  substituent. For compound **26** both crystallographically independent molecules are shown.

the  $C_a$ – $C_m$  bonds are significantly shorter and the  $C_a$ – $C_m$ – $C_a$  angles larger in the C5 quadrant than in the “phenyl” quadrants and are similar to values found for sterically unencumbered porphyrins. More evidence for a mixing of distortion modes is found in the structure of **45** (Figure 2). The overall conformation shows contributions of both *sad* and *ruf* distortions. The presence of the small cyano group results in overall smaller out-of-plane displacements of the pyrrole rings ( $\approx 20\%$  less) in the N23–C20–N24 part and is also evidenced by the large  $C_a$ –C15– $C_a$  angle of 124.2(4)°.

## Conclusion

These results clearly demonstrate that, by judicious use of organolithium reagents, it is possible to prepare nona-, deca-, undeca-, and dodecasubstituted porphyrins with almost any desired regiochemical pattern and combination of *meso* alkyl and aryl residues. The only requirements are appropriate planning of the reaction sequence, keeping in mind the different reactivities of LiR species (high for alkyl-lithium reagents with metalloporphyrins and high for arylli-

thium with free base porphyrins) and noting the preference for introduction of a second *meso* substituent at the *meso* position adjacent to that already carrying a residue (5,10-orientation). Careful selection of regiochemical positioning (e.g., 5,10 versus 5,15) and selection of the type of substituents (e.g.,  $sp^2$  versus  $sp^3$ ) offers significant opportunities for modulation of the conformation, and thus physicochemical properties, of these important biological cofactor mimics. As shown in Figure 7, the conformational trends observed in symmetric porphyrins are preserved (for example, as a rule of thumb, alkyl residues induced ruffling, aryl residues induced saddle distortion); however, a mixing of distortion modes now occurs. As targeted design of biomimetic porphyrins with specific conformations is now possible, further studies will be aimed at elucidating the exact interplay of substituents, distortion mode mixing, macrocycle conformation, and properties. The determination of the absolute structure of compound **26** indicates that it is possible to prepare nonplanar porphyrins with enantiotopic faces, and it will now be necessary to test whether it is possible to functionalize these porphyrins in such a way that specific binding of substrate molecules at one or both sides of the macrocycles becomes possible. If so, new avenues towards enantioselective catalysts or receptor molecules will be open.

## Experimental Section

**General Remarks:** All chemicals used were of analytical grade and were purchased from Aldrich Co. unless stated otherwise. THF was dried before use by distillation with sodium. All reactions with organolithium reagents were performed under a purified argon atmosphere. – Melting points were measured on a Büchi melting point apparatus and are uncorrected. – Silica gel 60 (Merck) was used for column chromatography. Analytical thin layer chromatography (TLC) was carried out using Merck 60 silica gel plates (precoated sheets, 0.2 mm thick, fluorescence indicator F254). –  $^1\text{H}$  NMR spectra were recorded at frequencies of 500 MHz (Bruker, AMX 500),  $^{13}\text{C}$  NMR spectra at 126 MHz. All chemical shifts are given in ppm, referenced on the  $\delta$  scale downfield from the TMS signal.  $\text{CDCl}_3$  was used as internal standard. – Electronic absorption spectra were recorded with a Specord S10 (Carl Zeiss Jena) spectrophotometer using dichloromethane as solvent. – Mass spectra were recorded with a Varian MAT 711 mass spectrometer using the EI technique with a direct insertion probe and, if not otherwise noted, with an excitation energy of 80 eV. – Elemental analyses were performed with a Perkin–Elmer 240 Analyzer. – Analytical HPLC was performed with an analytical column ( $2 \times 250$  nm.) filled with silica gel (Merck, Nucleosil 50) using a Knauer MPLC or HPLC pump. Solvent flow was 1 mL/min and porphyrins were detected at 350 nm using a UV detector.

**Metallation Reactions:** Octaethylporphyrin<sup>[38a]</sup> (**7**), its nickel(II) complex **8**,<sup>[38b]</sup> and **22**<sup>[26]</sup> were prepared according to standard procedures. Metal insertions were performed using the zinc(II) acetate method ( $\text{CH}_2\text{Cl}_2/35^\circ\text{C}$ ) for Zn(II) and the DMF method (DMF,  $153^\circ\text{C}$ ) or nickel(II) acetate for Ni<sup>II</sup>.<sup>[38b]</sup> Several mono-*meso*-substituted porphyrins were prepared using organolithium reagents as described by us previously.<sup>[19a]</sup>

**General Procedure A. – Butylation of Porphyrins:** Typically, a solution of the porphyrin in THF (ca 100 mg in 20 to 100 mL) was

cooled to  $-80^\circ\text{C}$  and treated dropwise with 3 to 4 equivalents of butyllithium (as a 2 M solution in cyclohexane). After stirring for 20 minutes at  $-80^\circ\text{C}$ , water (1 mL) was added and stirring continued for 5 min. Next, a solution of four equivalents of 2,3-dichloro-5,6-dicyano-1,4-benzoquinone (DDQ) in dichloromethane (ca. 0.06 M) was added, and the reaction mixture was stirred for a further 20 min at  $-60$  to  $-80^\circ\text{C}$ . After warming to room temperature, the mixture was filtered through a short plug of alumina (grade I). After evaporation of the solvent, the final purification involved column chromatography on alumina (grade III) followed by recrystallization from dichloromethane/*n*-hexane.

**General Procedure B. – Phenylation of Porphyrins:** A solution of the porphyrin in THF was treated at room temperature with 3 to 4 equivalents of phenyllithium (as a 1.8 M solution in cyclohexane). The mixture was heated to  $40^\circ\text{C}$  and stirred for 15 min. Next, the solution was cooled to  $0^\circ\text{C}$  followed by treatment and workup as described above in general procedure A.

**(5-*sec*-Butyl-2,3,7,8,12,13,17,18-octaethylporphyrinato)nickel(II) (11):** A solution of **8** (100 mg, 0.17 mmol) in 60 mL of THF was cooled to  $-35^\circ\text{C}$  and treated with *sec*-butyllithium (1.4 M solution, 0.3 mL, 0.55 mmol, 3 equiv.) as in procedure A. Column chromatography on neutral alumina (grade III), eluting with dichloromethane/hexane (1:6, v/v), yielded two fractions. The first (red) band gave 87 mg **11** (0.14 mmol, 82%, purple crystals) of the substituted porphyrin and the second minor one 11% of recovered starting material **8**. m.p.  $223^\circ\text{C}$ . –  $^1\text{H}$  NMR (500 MHz,  $\text{CDCl}_3$ ,  $\text{SiMe}_4$ ):  $\delta$  = 0.29 (t, 3 H,  $^3J$  = 7.1 Hz, *s*Bu- $\text{CHCH}_3$ ), 1.20 (m, 2 H, *s*Bu- $\text{CH}_2\text{CH}_3$ ), 1.68 (12 H, m,  $\text{CH}_2\text{CH}_3$ ), 1.75 (12 H, t,  $^3J$  = 7.5 Hz,  $\text{CH}_2\text{CH}_3$ ), 2.26 (d, 3 H,  $^3J$  = 3.4 Hz, *s*Bu- $\text{CHCH}_3$ ), 3.75 (16 H, m,  $\text{CH}_2\text{CH}_3$ ), 4.01 (m, 3 H, *s*Bu- $\text{CHCH}_2\text{CH}_3$ ), 9.22 (s, 2 H, 15-*H*), 9.25 (s, 1 H, 10-, 20-*H*). – UV/Vis ( $\text{CH}_2\text{Cl}_2$ ):  $\lambda_{\text{max}}$  (lg  $\epsilon$ ) = 412 (5.19), 538 (4.05), 573 nm (4.14). – MS (80 eV);  $m/z$  (%) = 646 (100) [ $\text{M}^+$ ], 617 (88) [ $\text{M}^+ - \text{C}_2\text{H}_5$ ], 590 (24) [ $\text{M}^+ - \text{C}_4\text{H}_9$ ], 323 (8) [ $\text{M}^{2+}$ ]. – HRMS: calcd. for  $\text{C}_{40}\text{H}_{52}\text{N}_4\text{Ni}$  646.3545; found 646.3572. – [ $\text{C}_{40}\text{H}_{52}\text{N}_4\text{Ni} \cdot 1/5\text{H}_2\text{O}$ , 649.96 g mol $^{-1}$ ]: calcd. C 74.26, H 8.11, N 8.67, found C 73.85, H 8.13, N 8.62.

**2,3,7,8,12,13,17,18-Octaethyl-5,10-diphenylporphyrin (14):** According to general procedure B, compound **10** (100 mg, 0.19 mmol) was dissolved in THF (60 mL) and treated with PhLi. Column chromatography on neutral alumina (grade III), eluting with dichloromethane/hexane (1:14, v/v), yielded two regioisomeric fractions and 3% of the starting material. The first (red) band gave 4 mg **20** (0.0058 mmol, 3%, purple crystals) and the third, major (green-brown) band gave 105 mg purple crystals (0.16 mmol, 84%) of **14**. m.p.  $223^\circ\text{C}$ . –  $^1\text{H}$  NMR (500 MHz,  $\text{CDCl}_3$ ,  $\text{SiMe}_4$ ):  $\delta$  = -2.68 (s, 2 H, br., *NH*), 0.40, 0.61, 1.52, 1.79 (24 H, each t,  $^3J$  = 7.5 Hz,  $\text{CH}_2\text{CH}_3$ ), 2.20, 2.66 (8 H, each m,  $\text{CH}_2\text{CH}_3$ ), 3.79, 3.91 (8 H, each q,  $^3J$  = 7.5 Hz,  $\text{CH}_2\text{CH}_3$ ), 7.59, 7.64 (6 H, each m,  $\text{H}_{\text{Ph}}$ ), 8.33 (d, 4 H,  $J$  = 4.3 Hz,  $\text{H}_{\text{Ph}}$ ), 9.62 (s, 2 H, 15-, 20-*H*). – UV/Vis ( $\text{CH}_2\text{Cl}_2$  + 1%  $\text{NEt}_3$ ):  $\lambda_{\text{max}}$  (lg  $\epsilon$ ) = 448 (5.22), 581 (3.86), 637 nm (3.42); ( $\text{CH}_2\text{Cl}_2$  + 1% TFA):  $\lambda_{\text{max}}$  (lg  $\epsilon$ ) = 456 (5.38), 642 nm (3.78). – MS (80 eV);  $m/z$  (%) = 686 (100) [ $\text{M}^+$ ], 671 (5) [ $\text{M}^+ - \text{CH}_3$ ], 657 (10) [ $\text{M}^+ - \text{C}_2\text{H}_5$ ], 609 (6) [ $\text{M}^+ - \text{C}_6\text{H}_5$ ], 534 (14) [ $\text{M}^+ - 2 \times \text{C}_6\text{H}_5$ ], 343 (18) [ $\text{M}^{2+}$ ]. – HRMS: calcd. for  $\text{C}_{48}\text{H}_{54}\text{N}_4$  686.4348; found 686.4379. – [ $\text{C}_{48}\text{H}_{54}\text{N}_4 \cdot \text{CH}_2\text{Cl}_2$ , 771.92 g mol $^{-1}$ ]: calcd. C 76.24, H 7.31, N 7.26, found C 26.21, H 7.16, N 7.26.

**(5,10-Dibutyl-2,3,7,8,12,13,17,18-octaethylporphyrinato)nickel(II) (15):** A solution of **8** (200 mg, 0.34 mmol) in THF (120 mL) was cooled to  $-70^\circ$  and treated with 0.8 mL of the BuLi stock solution. After stirring for 25 min at the same temperature, DDQ in abs. THF (15 mL of a 0.06 M solution) was added to the reaction

mixture and stirring was continued for another 30 min while the cold bath was removed. Finally, the solution was filtered through neutral alumina (grade I) and subjected to column chromatography on neutral alumina, eluting with ethyl acetate/hexane (1:50, v/v). The formation of four products was observed. After the starting material (9%), the next most polar band was identified as the monobutylated **12** (83 mg, 0.13 mmol, 38%). The other major (green) product was the 5,10-dibutylated nickel(II) complex **15** (62 mg, 0.082 mmol, 24%). The (orange) first and fourth bands were identified as mixtures of porphodimethenes (4%, 9%), which could not be characterized completely. Analytical data for the main products were identical to those obtained by a two-step ( $2 \times \text{BuLi}/\text{H}_2\text{O}/\text{DDQ}$ ) treatment of **8** with BuLi.<sup>[13a]</sup>

**(2,3,7,8,12,13,17,18-Octaethyl-5,10-diphenylporphyrinato)nickel(II) (16):** The nickel(II) complex was prepared by standard acetate methodology, using **14** (200 mg, 0.29 mmol) as starting material. Purification by column chromatography on alumina, eluting with dichloromethane/hexane (2:1, v/v), followed by recrystallization from  $\text{CH}_2\text{Cl}_2$ /methanol gave purple crystals of **16** (205 mg, 0.28 mmol, 97%). Alternatively, this porphyrin can be prepared by treatment of **13** with PhLi. However, yields are lower due to formation of polar side products. m.p. 260 °C. –  $^1\text{H}$  NMR (500 MHz,  $\text{CDCl}_3$ ,  $\text{SiMe}_4$ ):  $\delta$  = 0.49, 0.60, 1.46, 1.60 (24 H, each t,  $^3J$  = 7 Hz,  $\text{CH}_2\text{CH}_3$ ), 2.23, 2.48, 3.61, 3.72 (16 H, each q,  $^3J$  = 7.5 Hz,  $\text{CH}_2\text{CH}_3$ ), 7.59 (m, 4 H,  $\text{H}_{\text{Ph}}$ ), 7.64 (m, 2 H,  $\text{H}_{\text{Ph}}$ ), 8.02 (d, 4 H,  $J$  = 4 Hz,  $\text{H}_{\text{Ph}}$ ), 9.32 (s, 2 H, 15-, 20-*H*). – UV/Vis ( $\text{CH}_2\text{Cl}_2$ ):  $\lambda_{\text{max}}$  (lg  $\epsilon$ ) = 412 (5.08), 533 (3.91), 568 nm (3.05). – MS (80 eV);  $m/z$  (%) = 742 (100) [ $\text{M}^+$ ], 371 (35) [ $\text{M}^{2+}$ ]. – HRMS: calcd. for  $\text{C}_{48}\text{H}_{52}\text{N}_4\text{Ni}$  742.3545; found 742.3584. – [ $\text{C}_{48}\text{H}_{52}\text{N}_4\text{Ni} \cdot 1/2\text{H}_2\text{O}$ , 752.43 g mol $^{-1}$ ]: calcd. C 76.60, H 7.10, N 7.44, found C 76.80, H 7.13, N 7.25.

**(5-Butyl-2,3,7,8,12,13,17,18-octaethyl-10-phenylporphyrinato)-nickel(II) (17):** Treatment of **13** (100 mg, 0.15 mmol) in THF (60 mL) with BuLi, following general procedure A, with subsequent chromatography on neutral alumina, eluting with *n*-hexane/dichloromethane (7:1, v/v), and recrystallization from  $\text{CH}_2\text{Cl}_2$ /methanol, gave **17** as purple crystals, in 71% yield (76 mg, 0.11 mmol). In addition, 14% (15 mg, 0.02 mmol) of **23** was obtained. Alternatively, the title compound can be prepared by phenylation of **12** with PhLi. Treatment of **12** (100 mg, 0.15 mmol) in THF (40 mL) using general procedure B, followed by chromatography eluting with *n*-hexane/dichloromethane (4:1, v/v) and recrystallization, gave 72 mg (0.1 mmol, 67%) of **17** as the sole identifiable product. m.p. 237 °C. –  $^1\text{H}$  NMR (500 MHz,  $\text{CDCl}_3$ ,  $\text{SiMe}_4$ ):  $\delta$  = 0.49 (t, 3 H,  $^3J$  = 7.5 Hz,  $\text{CH}_2\text{CH}_2\text{CH}_2\text{CH}_3$ ), 0.60 (t, 3 H,  $^3J$  = 7.7 Hz,  $\text{CH}_2\text{CH}_3$ ), 0.90 (m, 4 H,  $\text{CH}_2\text{CH}_2\text{CH}_2\text{CH}_3$ ), 1.62–1.85 (18 H, m,  $^3J$  = 7.5 Hz,  $\text{CH}_2\text{CH}_3$ ), 1.86 (3 H, each t,  $^3J$  = 7.5 Hz,  $\text{CH}_2\text{CH}_3$ ), 2.53 (m, 4 H,  $\text{CH}_2\text{CH}_3$ ), 3.60 (12 H, m,  $\text{CH}_2\text{CH}_3$ ), 4.20 (m, 2 H,  $\text{CH}_2\text{CH}_2\text{CH}_2\text{CH}_3$ ), 7.58 (m, 5 H,  $\text{H}_{\text{Ph}}$ ), 9.09, 9.24 (2 H, each s, 15-, 20-*H*). – UV/Vis ( $\text{CH}_2\text{Cl}_2$ ):  $\lambda_{\text{max}}$  (lg  $\epsilon$ ) = 418 (5.17), 548 (3.62), 582 nm (2.54). – MS (80 eV);  $m/z$  (%) = 722 (100) [ $\text{M}^+$ ], 679 (8) [ $\text{M}^+ - \text{C}_3\text{H}_7$ ], 361 (12) [ $\text{M}^{2+}$ ]. – HRMS: calcd. for  $\text{C}_{46}\text{H}_{56}\text{N}_4\text{Ni}$  722.3858; found 722.3815.

**(2,3,7,8,12,13,17,18-Octaethyl-5,10-diphenylporphyrinato)zinc(II) (18):** The zinc(II) complex was prepared by the standard acetate methodology. For zinc(II) insertion, the corresponding free base **14** (200 mg, 0.29 mmol) was used. After purification by column chromatography (dichloromethane/hexane, 1:1, v/v) compound **18** (195 mg, 0.26 mmol, 90%) was obtained as purple crystals. m.p. 234 °C. –  $^1\text{H}$  NMR (500 MHz,  $\text{CDCl}_3$ ,  $\text{SiMe}_4$ ):  $\delta$  = 0.61, 0.75, 1.63, 1.82 (24 H, each t,  $^3J$  = 7 Hz,  $\text{CH}_2\text{CH}_3$ ), 2.42, 2.60 (8 H, each q,  $^3J$  = 7 Hz,  $\text{CH}_2\text{CH}_3$ ), 3.90 (m, 8 H,  $^3J$  = 7 Hz,  $\text{CH}_2\text{CH}_3$ ),

7.59 (t, 4 H,  $^3J$  = 7 Hz,  $\text{H}_{\text{Ph}}$ ), 7.70 (d, 2 H,  $J$  = 4 Hz,  $\text{H}_{\text{Ph}}$ ), 8.26 (d, 6 H,  $J$  = 4 Hz,  $\text{H}_{\text{Ph}}$ ), 9.76 (s, 2 H, 15-, 20-*H*). – UV/Vis ( $\text{CH}_2\text{Cl}_2$ ):  $\lambda_{\text{max}}$  (lg  $\epsilon$ ) = 419 (5.33), 548 (3.76), 5.82 nm (3.52). – MS (80 eV);  $m/z$  (%) = 748 (100) [ $\text{M}^+$ ], 374 (9) [ $\text{M}^{2+}$ ]. – HRMS: calcd. for  $\text{C}_{48}\text{H}_{52}\text{N}_4\text{Zn}$  748.34834; found 748.34399. – [ $\text{C}_{48}\text{H}_{52}\text{N}_4\text{Zn}$ , 748.34 g mol $^{-1}$ ]: calcd. C 76.97, H 7.00, N 7.48, found C 77.09, H 7.02, N 7.43.

**2,3,7,8,12,13,17,18-Octaethyl-5,15-diphenylporphyrin (20):** Obtained as a side product during the synthesis of **14**, in 3% yield. – Crystal data: The compound crystallized in the monoclinic space group  $P2_1/n$ ,  $a$  = 14.599(5),  $b$  = 15.717(4),  $c$  = 17.372(6) Å,  $\beta$  = 105.51(2)°,  $V$  = 3841(2) Å $^3$ ,  $Z$  = 4.

**(5-Butyl-2,3,7,8,12,13,17,18-octaethyl-15-phenylporphyrinato)-nickel(II) (23):** This compound was obtained as a side product in the synthesis of **17** by treatment of **13** with BuLi. m.p. 252 °C. –  $^1\text{H}$  NMR (500 MHz,  $\text{CDCl}_3$ ,  $\text{SiMe}_4$ ):  $\delta$  = 0.58 (t, 3 H,  $^3J$  = 7.4 Hz,  $\text{CH}_2\text{CH}_2\text{CH}_2\text{CH}_3$ ), 0.78 (m, 4 H,  $\text{CH}_2\text{CH}_2\text{CH}_2\text{CH}_3$ ), 0.90 (t, 6 H,  $^3J$  = 7.4 Hz,  $\text{CH}_2\text{CH}_3$ ), 1.60 (12 H, t,  $^3J$  = 7.5 Hz,  $\text{CH}_2\text{CH}_3$ ), 1.81 (t, 6 H,  $^3J$  = 7.3 Hz,  $\text{CH}_2\text{CH}_3$ ), 2.60 (m, 4 H,  $\text{CH}_2\text{CH}_3$ ), 3.51–3.84 (12 H, m,  $\text{CH}_2\text{CH}_3$ ), 4.30 (m, 2 H,  $\text{CH}_2\text{CH}_2\text{CH}_2\text{CH}_3$ ), 7.35–7.69 (m, 5 H,  $\text{H}_{\text{Ph}}$ ), 9.18 (s, 2 H, 10-, 20-*H*). – UV/Vis ( $\text{CH}_2\text{Cl}_2$ ):  $\lambda_{\text{max}}$  (lg  $\epsilon$ ) = 418 (5.25), 535 (4.02), 572 nm (3.82). – MS (80 eV);  $m/z$  (%) = 722 (100) [ $\text{M}^+$ ], 679 (11) [ $\text{M}^+ - \text{C}_3\text{H}_7$ ], 665 (4) [ $\text{M}^+ - \text{C}_4\text{H}_9$ ], 361 (13) [ $\text{M}^{2+}$ ]. – HRMS: calcd. for  $\text{C}_{46}\text{H}_{56}\text{N}_4\text{Ni}$  722.3858; found 722.3823. – [ $\text{C}_{46}\text{H}_{56}\text{N}_4\text{Ni} \cdot 1/5\text{H}_2\text{O}$ , 725.99 g mol $^{-1}$ ]: calcd. C 76.41, H 7.81, N 7.75, found C 76.03, H 7.83, N 7.72.

**2,3,7,8,12,13,17,18-Octaethyl-5,10,15-triphenylporphyrin (24):** Compound **20** (100 mg, 0.15 mmol) was dissolved in THF (50 mL) and treated under the conditions given under procedure B. Final purification was achieved by column chromatography on alumina, using dichloromethane/*n*-hexane (1:5, v/v) as eluent. The major (green) band was identified as the desired product; recrystallization from  $\text{CH}_2\text{Cl}_2$ /methanol gave 80 mg (0.10 mmol, 70%) of purple crystals. m.p. 219 °C. –  $^1\text{H}$  NMR (500 MHz,  $\text{CDCl}_3$ ,  $\text{SiMe}_4$ ):  $\delta$  = –2.11 (s, 2 H, br., *NH*), 0.42, 0.50, 0.76, 1.55 (24 H, each t,  $^3J$  = 7.6 Hz,  $\text{CH}_2\text{CH}_3$ ), 2.23 (m, 8 H,  $\text{CH}_2\text{CH}_3$ ), 2.74, 3.75 (8 H, each q,  $^3J$  = 7.6 Hz,  $\text{CH}_2\text{CH}_3$ ), 7.66 (m, 9 H,  $\text{H}_{\text{Ph}}$ ), 8.33 (d, 4 H,  $^3J$  = 4.2 Hz,  $\text{H}_{\text{Ph}}$ ), 8.38 (d, 2 H,  $^3J$  = 4.3 Hz,  $\text{H}_{\text{Ph}}$ ), 9.39 (s, 1 H, 20-*H*). – UV/Vis ( $\text{CH}_2\text{Cl}_2$ ):  $\lambda_{\text{max}}$  (lg  $\epsilon$ ) = 450 (5.17), 534 (3.18), 580 (3.32), 635 nm (2.45). – MS (80 eV);  $m/z$  (%) = 762 (100) [ $\text{M}^+$ ], 733 (15) [ $\text{M}^+ - \text{C}_2\text{H}_5$ ], 685 (10) [ $\text{M}^+ - \text{C}_6\text{H}_5$ ], 381 (14) [ $\text{M}^{2+}$ ]. – HRMS: calcd. for  $\text{C}_{54}\text{H}_{58}\text{N}_4$  762.4661; found 762.4583.

**(2,3,7,8,12,13,17,18-Octaethyl-5,10,15-triphenylporphyrinato)-nickel(II) (25):** This compound was prepared by metallation of **24** with nickel(II) acetate in DMF. Purification was by column chromatography on alumina, eluting with dichloromethane/*n*-hexane (1:3, v/v), and gave 68 mg (0.083 mmol) of purple crystals. m.p. 235 °C. –  $^1\text{H}$  NMR (500 MHz,  $\text{SiMe}_4$ ):  $\delta$  = 0.38 (12 H, m,  $\text{CH}_2\text{CH}_3$ ), 0.64, 1.40 (12 H, each t,  $^3J$  = 7.5 Hz,  $\text{CH}_2\text{CH}_3$ ), 2.19 (m, 8 H,  $\text{CH}_2\text{CH}_3$ ), 2.22, 3.54 (8 H, each q,  $^3J$  = 7.5 Hz,  $\text{CH}_2\text{CH}_3$ ), 7.60 (m, 6 H,  $\text{H}_{\text{Ph}}$ ), 8.05 (d, 9 H,  $^3J$  = 4 Hz,  $\text{H}_{\text{Ph}}$ ), 9.22 (s, 1 H, 20-*H*). – UV/Vis ( $\text{CH}_2\text{Cl}_2$ ):  $\lambda_{\text{max}}$  (lg  $\epsilon$ ) = 418 (4.92), 543 (3.78), 579 nm (3.73). – MS (80 eV);  $m/z$  (%) = 818 (100) [ $\text{M}^+$ ], 409 (16) [ $\text{M}^{2+}$ ]. – HRMS: calcd. for  $\text{C}_{54}\text{H}_{56}\text{N}_4\text{Ni}$  818.3859; found 818.3813.

**(5-Butyl-2,3,7,8,12,13,17,18-octaethyl-10,20-diphenylporphyrinato)-nickel(II) (26):** Compound **22** (100 mg, 0.13 mmol) in THF (80 mL) was cooled to –80 °C and the BuLi stock solution (0.4 mL) was added. After stirring for 20 min,  $\text{H}_2\text{O}$  (1 mL) in THF (10 mL) was added to the reaction mixture and stirring was continued for 10 min. The cooling bath was removed, followed by the addition of a solution of DDQ (9 mL, 0.06 M). Subsequent steps were as



described in procedure A. Final purification was by chromatography on alumina, eluting with dichloromethane/*n*-hexane (1:15, v/v). The first, minor (red) band was identified by electronic absorption spectroscopy as a porphodimethene. The main product eluted as the second (green) band and gave 62 mg (0.078 mmol, 60%) purple crystals after recrystallization from CH<sub>2</sub>Cl<sub>2</sub>/methanol. m.p. 265 °C. – <sup>1</sup>H NMR (500 MHz, CDCl<sub>3</sub>, SiMe<sub>4</sub>): δ = 0.68 (t, 3 H, <sup>3</sup>J = 7.5 Hz, CH<sub>2</sub>CH<sub>2</sub>CH<sub>2</sub>CH<sub>3</sub>), 1.05 (m, 4 H, CH<sub>2</sub>CH<sub>2</sub>CH<sub>2</sub>CH<sub>3</sub>), 0.66, 0.70, 1.59, 1.66 (24 H, each t, <sup>3</sup>J = 7.5 Hz, CH<sub>2</sub>CH<sub>3</sub>), 2.45 (m, 8 H, CH<sub>2</sub>CH<sub>3</sub>), 3.48, 3.57 (8 H, each m, CH<sub>2</sub>CH<sub>3</sub>), 4.08 (m, 2 H, CH<sub>2</sub>CH<sub>2</sub>CH<sub>2</sub>CH<sub>3</sub>), 7.50 (m, 4 H, br., H<sub>Ph</sub>), 7.62 (m, 2 H, H<sub>Ph</sub>), 8.04 (m, 4 H, br., H<sub>Ph</sub>), 9.03 (s, 1 H, 20-H). – UV/Vis (CH<sub>2</sub>Cl<sub>2</sub>): λ<sub>max</sub> (lg ε) = 423 (4.90), 543 (3.81), 579 nm (3.85). – MS (80 eV); *m/z* (%) = 798 (100) [M<sup>+</sup>], 755 (9) [M<sup>+</sup> – C<sub>3</sub>H<sub>7</sub>], 399 (17) [M<sup>2+</sup>]. – HRMS: calcd. for C<sub>52</sub>H<sub>60</sub>N<sub>4</sub>Ni 798.41877; found 798.41714 (HRMS). – [C<sub>52</sub>H<sub>60</sub>N<sub>4</sub>Ni·1/5H<sub>2</sub>O, 802.02 g mol<sup>–1</sup>]: calcd. C 78.15, H 7.57, N 7.02, found C 78.12, H 7.62, N 7.01.

**(5,15-Dibutyl-2,3,7,8,12,13,17,18-octaethyl-10-phenylporphyrinato)-nickel(II) (27):** A solution of **17** (100 mg, 0.14 mmol) in THF (45 mL) was cooled to –100 °C, treated with the BuLi stock solution (0.4 mL), stirred for 20 min and then diluted with a mixture of H<sub>2</sub>O (1 mL) in THF (10 mL). After stirring for a further 10 min and removal of the cold bath, a solution of DDQ in THF (8 mL of 0.06 M) was added immediately and stirring was continued for 10 min. Further workup was according to procedure A. Column chromatography on alumina, eluting with neat *n*-hexane, gave three fractions. The first fraction was identified as a mixture of porphodimethenes that could not be separated further. The major, second (green) band gave 72 mg (0.092 mmol, 65%) of **27** after recrystallization from CH<sub>2</sub>Cl<sub>2</sub>/methanol. The last (green) band was identified after crystallization from CH<sub>2</sub>Cl<sub>2</sub>/methanol as the regioisomeric compound **30** (5 mg, 6.4 μmol, 4%, see below).

Alternatively, compound **27** can be prepared by phenylation of the 5,15-dibutyl precursor **21**. For this, **21** (100 mg, 0.15 mmol) was dissolved in THF (100 mL) and treated with PhLi, following procedure B. Final purification was achieved by column chromatography on alumina, using *n*-hexane as eluent. The porphyrin was obtained as purple crystals (64 mg, 0.041 mmol, 27% yield). m.p. 238 °C. – <sup>1</sup>H NMR (500 MHz, CDCl<sub>3</sub>, SiMe<sub>4</sub>): δ = 0.55, 0.80, 1.65, 1.71, 1.80 (24 H, each t, <sup>3</sup>J = 7.5 Hz, CH<sub>2</sub>CH<sub>3</sub>), 0.82 (m, 6 H, CH<sub>2</sub>CH<sub>2</sub>CH<sub>2</sub>CH<sub>3</sub>), 1.00 (m, 8 H, CH<sub>2</sub>CH<sub>2</sub>CH<sub>2</sub>CH<sub>3</sub>), 2.35 (m, 4 H, CH<sub>2</sub>CH<sub>3</sub>), 3.62 (12 H, m, CH<sub>2</sub>CH<sub>3</sub>), 4.11 (m, 4 H, CH<sub>2</sub>CH<sub>2</sub>CH<sub>2</sub>CH<sub>3</sub>), 7.30 (m, 2 H, H<sub>Ph</sub>), 7.66 (m, 3 H, H<sub>Ph</sub>), 8.80 (s, 1 H, 20-H). – UV/Vis (CH<sub>2</sub>Cl<sub>2</sub>): λ<sub>max</sub> (lg ε) = 432 (4.91), 562 (3.71), 607 nm (3.36). – MS (80 eV); *m/z* (%) = 778 (100) [M<sup>+</sup>], 735 (12) [M<sup>+</sup> – C<sub>3</sub>H<sub>7</sub>], 389 (33) [M<sup>2+</sup>]. – HRMS: calcd. for C<sub>50</sub>H<sub>64</sub>N<sub>4</sub>Ni 778.4484; found 778.4445.

**(5-Butyl-2,3,7,8,12,13,17,18-octaethyl-10,15-phenylporphyrinato)-nickel(II) (29):** Compound **16** (100 mg, 0.13 mmol) in THF (40 mL) was treated with the BuLi stock solution (0.5 mL) according to procedure A. After stirring for 10 min, a mixture of H<sub>2</sub>O (1 mL) and THF (10 mL) was added, and stirring was continued for 5 min. The cooling bath was removed and DDQ (9 mL of a 0.06 M solution in THF) was added. Final purification was by column chromatography, eluting with neat *n*-hexane, and gave three fractions. The second, major band was identified as the desired product (57%, 59 mg, 0.074 mmol, purple crystals from CH<sub>2</sub>Cl<sub>2</sub>/methanol). The third band consisted of 6 mg (6%) recovered starting material. The first (orange) band exhibited a UV/Vis spectrum typical of a porphodimethene (443, 557 nm). Recrystallization of this band gave 22 mg of dark brown crystals. Further chromatographic separation

of this material (alumina, neat hexane) revealed the presence of three different hydroporphyrins. The yield of the first, very faint band was too low for identification. The second (red) band was identified as **33** (8%), while the third, major (red) band was identified as **32** (12%) (analytical data see below). Compound **29** was also obtained as the main product of the butylation of **16** without addition of water. For this reaction, **16** (100 mg, 0.13 mmol) was dissolved in THF (30 mL) and treated with BuLi (1 mmol) at –80 °C. After stirring for 15 min, the cold bath was removed and DDQ (9 mL of a 0.06 M solution in THF). Final purification was by column chromatography, eluting with neat *n*-hexane, and gave three fractions. The second, major band was identified as compound **29** (61%, 63 mg, 0.079 mmol, purple crystals from CH<sub>2</sub>Cl<sub>2</sub>/methanol). The first, minor (orange) band and the third band consisted of porphodimethenes, as indicated by their UV/Vis spectra. Complete characterization of these side products was not possible. Analytical data for **29** are: m.p. 260 °C. – <sup>1</sup>H NMR (500 MHz, CDCl<sub>3</sub>, SiMe<sub>4</sub>): δ = 0.34, 0.47, 0.75, 0.80, 0.90 (15 H, t, <sup>3</sup>J = 7.5 Hz, 4 × CH<sub>2</sub>CH<sub>3</sub>, CH<sub>2</sub>CH<sub>2</sub>CH<sub>2</sub>CH<sub>3</sub>), 1.16, 1.30 (m, 4 H, CH<sub>2</sub>CH<sub>2</sub>CH<sub>2</sub>CH<sub>3</sub>), 1.46, 1.59, 1.68, 1.77 (12 H, each t, <sup>3</sup>J = 7.5 Hz, CH<sub>2</sub>CH<sub>3</sub>), 2.23–2.48 (m, 8 H, CH<sub>2</sub>CH<sub>3</sub>), 3.33–3.45 (m, 2 H, CH<sub>2</sub>CH<sub>3</sub>), 3.46–3.60 (m, 4 H, CH<sub>2</sub>CH<sub>3</sub>), 3.65 (q, 2 H, <sup>3</sup>J = 7.3 Hz, CH<sub>2</sub>CH<sub>3</sub>), 4.21 (m, 2 H, br., CH<sub>2</sub>CH<sub>2</sub>CH<sub>2</sub>CH<sub>3</sub>), 7.50 (m, 4 H, H<sub>Ph</sub>), 7.62 (m, 2 H, H<sub>Ph</sub>), 7.96 (m, 4 H, br., H<sub>Ph</sub>), 9.00 (s, 1 H, 20-H). – UV/Vis (CH<sub>2</sub>Cl<sub>2</sub>): λ<sub>max</sub> (lg ε) = 426 (4.87), 551 (3.79), 590 nm (3.78). – MS (80 eV); *m/z* (%) = 798 (100) [M<sup>+</sup>], 755 (15) [M<sup>+</sup> – C<sub>3</sub>H<sub>7</sub>], 399 (35) [M<sup>2+</sup>]. – HRMS: calcd. for C<sub>52</sub>H<sub>60</sub>N<sub>4</sub>Ni 798.4172; found 798.4126. – [C<sub>52</sub>H<sub>60</sub>N<sub>4</sub>Ni·1/5H<sub>2</sub>O, 802.02 g mol<sup>–1</sup>]: calcd. C 78.15, H 7.57, N 7.02, found C 78.12, H 7.62, N 7.01.

**(5,10-Dibutyl-2,3,7,8,12,13,17,18-octaethyl-15-phenylporphyrinato)-nickel(II) (30):** This compound was obtained as a side product during the synthesis of **27**. Yield: 5 mg purple crystals (6.4 μmol, 5%) of **30**. m.p. 236 °C. – <sup>1</sup>H NMR (500 MHz, CDCl<sub>3</sub>, SiMe<sub>4</sub>): δ = 0.59 (t, 6 H, CH<sub>2</sub>CH<sub>2</sub>CH<sub>2</sub>CH<sub>3</sub>), 0.78 (m, 4 H, CH<sub>2</sub>CH<sub>2</sub>CH<sub>2</sub>CH<sub>3</sub>), 1.13 (m, 4 H, CH<sub>2</sub>CH<sub>2</sub>CH<sub>2</sub>CH<sub>3</sub>), 1.71–1.98 (24 H, m, CH<sub>2</sub>CH<sub>3</sub>), 2.39 (m, 4 H, CH<sub>2</sub>CH<sub>3</sub>), 3.57 (12 H, m, CH<sub>2</sub>CH<sub>3</sub>), 4.08 (m, 4 H, CH<sub>2</sub>CH<sub>2</sub>CH<sub>2</sub>CH<sub>3</sub>), 7.46 (m, 2 H, H<sub>Ph</sub>), 7.56 (m, 3 H, H<sub>Ph</sub>), 8.84 (s, 1 H, 20-H). – UV/Vis (CH<sub>2</sub>Cl<sub>2</sub>): λ<sub>max</sub> (lg ε) = 434 (5.90), 562 (4.47), 606 nm (3.97). – MS (80 eV); *m/z* (%) = 778 (100) [M<sup>+</sup>], 735 (21) [M<sup>+</sup> – C<sub>3</sub>H<sub>7</sub>], 389 (8) [M<sup>2+</sup>]. – HRMS: calcd. for C<sub>50</sub>H<sub>64</sub>N<sub>4</sub>Ni 778.4484; found 778.4473.

**(2,3,7,8,12,13,17,18-Octaethyl-5-hexyl-10,15-phenylporphyrinato)-nickel(II) (31):** A solution of **16** (100 mg, 0.13 mmol) in THF (30 mL) was treated with hexyllithium (0.5 mmol), in a manner corresponding to procedure A. After stirring for 10 min, the reaction mixture was hydrolyzed with water (1 mL). The cold bath was removed and DDQ (9 mL of a 0.06 M solution) in THF was added. Final purification was by column chromatography, eluting with neat *n*-hexane, and gave two fractions. The second, major band was identified as the title compound **31** (62%, 67 mg, 0.081 mmol, purple crystals from CH<sub>2</sub>Cl<sub>2</sub>/CH<sub>3</sub>OH). The first, minor (orange) band consisted of an as yet uncharacterized porphodimethene as indicated by its UV/Vis-spectrum. Use of the same reaction procedure, but with omission of the hydrolysis step, gave 60% of **31** and two unidentified porphodimethenes. Analytical data for **31** are: m.p. 260 °C. – <sup>1</sup>H NMR (500 MHz, CDCl<sub>3</sub>, SiMe<sub>4</sub>): δ = 0.29, 0.40, 0.65, 0.72, 0.83 (15 H, t, <sup>3</sup>J = 7.5 Hz, CH<sub>2</sub>CH<sub>2</sub>CH<sub>2</sub>CH<sub>2</sub>CH<sub>2</sub>CH<sub>3</sub>, 4 × CH<sub>2</sub>CH<sub>3</sub>), 1.00–1.40 (m, 8 H, CH<sub>2</sub>CH<sub>2</sub>CH<sub>2</sub>CH<sub>2</sub>CH<sub>2</sub>CH<sub>3</sub>), 1.40, 1.52, 1.63, 1.80 (12 H, each t, <sup>3</sup>J = 7.5 Hz, CH<sub>2</sub>CH<sub>3</sub>), 2.21–2.55 (m, 8 H, CH<sub>2</sub>CH<sub>3</sub>), 3.41 (m, 2 H, CH<sub>2</sub>CH<sub>3</sub>), 3.55 (m, 4 H, CH<sub>2</sub>CH<sub>3</sub>), 3.69 (m, 2 H, CH<sub>2</sub>CH<sub>3</sub>),



4.22 (m, br., 2 H,  $\text{CH}_2\text{CH}_2\text{CH}_2\text{CH}_2\text{CH}_2\text{CH}_3$ ), 7.50 (m, 4 H,  $\text{H}_{\text{Ph}}$ ), 7.63 (m, 2 H,  $\text{H}_{\text{Ph}}$ ), 7.80–8.13 (m, 4 H, br.,  $\text{H}_{\text{Ph}}$ ), 9.00 (s, 1 H, 20-*H*). – UV/Vis ( $\text{CH}_2\text{Cl}_2$ ):  $\lambda_{\text{max}}$  (lg  $\epsilon$ ) = 426 (4.87), 551 (3.79), 590 nm (3.78). – MS (80 eV);  $m/z$  (%) = 826 (100) [ $\text{M}^+$ ], 413 (24) [ $\text{M}^{2+}$ ]. – HRMS: calcd. for  $\text{C}_{54}\text{H}_{64}\text{N}_4\text{Ni}$  826.44845; found 826.44397.

**(5-Butyl-2,3,7,8,12,13,17,18-octaethyl-5,15-dihydro-10,15-diphenylporphyrinato)nickel(II) (32):** This compound was obtained during the synthesis of **29**. Final purification of the porphodimethene fraction required a second column chromatographic separation (alumina grade III, neat hexane) and gave three bands. The last (red) band was identified as **32**, which was obtained as dark-brown crystals (12 mg, 0.015 mmol, 12%) after recrystallization from  $\text{CH}_2\text{Cl}_2$ /methanol. m.p. 211 °C. –  $^1\text{H}$  NMR (500 MHz,  $\text{CDCl}_3$ ,  $\text{SiMe}_4$ ):  $\delta$  = 0.51 (t, 3 H,  $^3J$  = 7.5 Hz,  $\text{CH}_2\text{CH}_2\text{CH}_2\text{CH}_3$ ), 1.01–1.50 (28 H, m,  $\text{CH}_2\text{CH}_2\text{CH}_2\text{CH}_3$ ,  $4 \times \text{CH}_2\text{CH}_3$ ), 2.13 (m, 4 H,  $\text{CH}_2\text{CH}_3$ ), 2.29 (m, 4 H,  $\text{CH}_2\text{CH}_3$ ), 2.49 (m, 8 H,  $\text{CH}_2\text{CH}_3$ ), 3.00 (m, 2 H,  $\text{CH}_2\text{CH}_2\text{CH}_2\text{CH}_3$ ), 3.75 (t, 1 H,  $^3J$  = 7.5 Hz, 5-*H*), 5.22 (s, 1 H, 15-*H*), 6.61 (s, 1 H, 20-*H*), 7.38–7.54 (m, 6 H,  $\text{H}_{\text{Ph}}$ ), 7.96 (d, 4 H,  $\text{H}_{\text{Ph}}$ ). – UV/Vis ( $\text{CH}_2\text{Cl}_2$ ):  $\lambda_{\text{max}}$  (lg  $\epsilon$ ) = 443 (4.61), 546 nm (4.23). – MS (80 eV);  $m/z$  (%) = 800 (71) [ $\text{M}^+$ ], 743 (100) [ $\text{M}^+ - \text{C}_4\text{H}_9$ ], 714 (28) [ $\text{M}^+ - \text{C}_2\text{H}_5$ ], 400 (5) [ $\text{M}^{2+}$ ]. – HRMS: calcd. for  $\text{C}_{52}\text{H}_{62}\text{N}_4\text{Ni}$  800.4328; found 800.43279.

**(5,10-Butyl-2,3,7,8,12,13,17,18-octaethyl-5,10-dihydro-15,20-diphenylporphyrinato)nickel(II) (37):** This compound was obtained during the synthesis of **29**. The second (red) band obtained upon chromatography of the porphodimethene fraction was identified as **33** (9 mg, 0.01 mmol, 0.8%, dark brown crystals). m.p. 211 °C. –  $^1\text{H}$  NMR (500 MHz,  $\text{CDCl}_3$ ,  $\text{SiMe}_4$ ):  $\delta$  = 0.53 (t, 6 H,  $^3J$  = 7.5 Hz,  $\text{CH}_2\text{CH}_2\text{CH}_2\text{CH}_3$ ), 0.95 (18 H, m,  $\text{CH}_2\text{CH}_3$ ), 1.10 (m, 6 H,  $2 \times \text{CH}_2\text{CH}_3$ ), 1.50 (m, 4 H,  $\text{CH}_2\text{CH}_2\text{CH}_2\text{CH}_3$ ), 1.82 (m, 4 H,  $\text{CH}_2\text{CH}_2\text{CH}_2\text{CH}_3$ ), 2.13 (m, 4 H,  $\text{CH}_2\text{CH}_3$ ), 2.27 (m, 8 H,  $\text{CH}_2\text{CH}_3$ ), 2.60 (m, 4 H,  $\text{CH}_2\text{CH}_3$ ), 3.02 (m, 4 H,  $\text{CH}_2\text{CH}_2\text{CH}_2\text{CH}_3$ ), 3.77 (t, 2 H,  $^3J$  = 7.5 Hz, 5-, 10-*H*), 5.22 (t, 1 H,  $^3J$  = 7.5 Hz, 15-*H*), 6.61 (s, 1 H, 20-*H*), 7.41–7.60 (m, 6 H,  $\text{H}_{\text{Ph}}$ ), 8.50 (d, 4 H,  $\text{H}_{\text{Ph}}$ ). – UV/Vis ( $\text{CH}_2\text{Cl}_2$ ):  $\lambda_{\text{max}}$  (lg  $\epsilon$ ) = 449 (4.60), 548 nm (3.79). – MS (80 eV);  $m/z$  (%) = 856 (91) [ $\text{M}^+$ ], 799 (100) [ $\text{M}^+ - \text{C}_4\text{H}_9$ ], 428 (5) [ $\text{M}^{2+}$ ]. – HRMS: calcd. for  $\text{C}_{56}\text{H}_{70}\text{N}_4\text{Ni}$  856.4554; found 856.4461.

**(5-Butyl-2,3,7,8,12,13,17,18-octaethyl-10,15,20-phenylporphyrinato)nickel(II) (34):** A solution of **25** (100 mg, 0.11 mmol) in THF (20 mL) was treated at –100 °C with BuLi (0.5 mmol) according to procedure A. Chromatography on neutral alumina (grade III, neat hexane) gave ≈28% of a mixture of porpho(d)i-methenes and 47% (48 mg, 5.3  $\mu\text{mol}$ ) of the desired product **34** after crystallization from  $\text{CH}_2\text{Cl}_2$ /methanol. m.p. 258 °C. –  $^1\text{H}$  NMR (500 MHz,  $\text{CDCl}_3$ ,  $\text{SiMe}_4$ ):  $\delta$  = 0.49 (m, 9 H,  $2 \times \text{CH}_2\text{CH}_3$ ,  $\text{CH}_2\text{CH}_2\text{CH}_2\text{CH}_3$ ), 0.81 (12 H, t,  $\text{CH}_2\text{CH}_3$ ), 1.11 (m, 4 H,  $\text{CH}_2\text{CH}_2\text{CH}_2\text{CH}_3$ ), 1.38 (t, 6 H,  $\text{CH}_2\text{CH}_3$ ), 2.20 (12 H, m,  $\text{CH}_2\text{CH}_3$ ), 3.10 (m, 4 H,  $\text{CH}_2\text{CH}_3$ ), 3.72 (m, 2 H,  $\text{CH}_2\text{CH}_2\text{CH}_2\text{CH}_3$ ), 7.40–7.99 (15 H, m,  $\text{H}_{\text{Ph}}$ ). – UV/Vis ( $\text{CH}_2\text{Cl}_2$ ):  $\lambda_{\text{max}}$  (lg  $\epsilon$ ) = 435 (4.93), 553 (3.72), 595 (3.64) nm. – MS (80 eV);  $m/z$  (%) = 834 (100) [ $\text{M}^+$ ], 792 (17) [ $\text{M}^+ - \text{C}_3\text{H}_7$ ], 777 (59) [ $\text{M}^+ - \text{C}_4\text{H}_9$ ], 417 (16) [ $\text{M}^{2+}$ ]. – HRMS: calcd. for  $\text{C}_{58}\text{H}_{64}\text{N}_4\text{Ni}$  834.5153; found 834.51105. – [ $\text{C}_{58}\text{H}_{64}\text{N}_4\text{Ni} \cdot 1/5\text{H}_2\text{O}$ , 878.05 g  $\text{mol}^{-1}$ ]; calcd. C 79.59, H 7.38, N 6.41, found C 79.21, H 7.38, N 6.37.

**(5,10-Dibutyl-2,3,7,8,12,13,17,18-octaethyl-15,20-diphenylporphyrinato)nickel(II) (35):** A solution of **29** (100 mg, 0.13 mmol) in THF (35 mL) was cooled to –100 °C and mixed with the BuLi stock solution (0.25 mL). After stirring for 10 min a mixture of

$\text{H}_2\text{O}$  (1 mL) and THF (10 mL) was added and stirring was continued for 5 min. The cold bath was removed, followed by the addition of DDQ (8 mL of 0.06 M solution) in THF. Subsequent steps were as in general procedure A. Column chromatography on alumina, eluting with neat hexane, gave a first (orange) fraction, followed by the major fraction and starting material (5%). The orange fraction possessed a UV/Vis spectrum typical of a porphodimethene. NMR spectroscopy indicated a mixture of compounds that could not be separated chromatographically. Recrystallization of the major fraction from  $\text{CH}_2\text{Cl}_2$ /methanol gave 53 mg purple crystals (0.062 mmol, 48%) of **35**. m.p. 243 °C. –  $^1\text{H}$  NMR (500 MHz,  $\text{CDCl}_3$ ,  $\text{SiMe}_4$ ):  $\delta$  = 0.53 (12 H, m,  $2 \times \text{CH}_2\text{CH}_3$ ,  $2 \times \text{CH}_2\text{CH}_2\text{CH}_2\text{CH}_3$ ), 0.80 (m, 8 H,  $\text{CH}_2\text{CH}_2\text{CH}_2\text{CH}_3$ ), 1.36, 1.50, 1.60 (18 H, m,  $\text{CH}_2\text{CH}_3$ ), 2.23, 2.36, 3.29, 3.40 (16 H, m,  $\text{CH}_2\text{CH}_3$ ), 4.01 (m, 4 H,  $\text{CH}_2\text{CH}_2\text{CH}_2\text{CH}_3$ ), 7.50 (m, 4 H,  $\text{H}_{\text{Ph}}$ ), 7.55 (m, 2 H,  $\text{H}_{\text{Ph}}$ ), 7.88 (m, 4 H, br.,  $\text{H}_{\text{Ph}}$ ). – UV/Vis ( $\text{CH}_2\text{Cl}_2$ ):  $\lambda_{\text{max}}$  (lg  $\epsilon$ ) = 438 (4.90), 562 (3.85), 601 nm (3.68). – MS (80 eV);  $m/z$  (%) = 854 (100) [ $\text{M}^+$ ], 826 (4) [ $\text{M}^+ - \text{C}_2\text{H}_4$ ], 811 (10) [ $\text{M}^+ - \text{C}_3\text{H}_7$ ], 799 (13) [ $\text{M}^+ - \text{C}_4\text{H}_7$ ], 427 (21) [ $\text{M}^{2+}$ ]. – HRMS: calcd. for  $\text{C}_{56}\text{H}_{68}\text{N}_4\text{Ni}$  854.4797; found 854.4764.

**(5,15-Dibutyl-2,3,7,8,12,13,17,18-octaethyl-10,20-diphenylporphyrinato)nickel(II) (36):** A solution of **26** (100 mg, 0.13 mmol) in THF (30 mL) was cooled to –100 °C and BuLi stock solution (0.2 mL, 0.4 mmol) was added. After stirring for 5 min, a mixture of  $\text{H}_2\text{O}$  (1 mL) and THF (10 mL) was added, and stirring was continued for 5 min. Next, the cooling bath was removed, followed by the addition of DDQ (10 mL of a 0.6 M solution). Subsequent steps were as described in general procedure A. Final column chromatography used alumina, eluting with neat hexane. The first fraction contained a small amount of a porphodimethene (**40**) and was followed by the major band containing the product. This product fraction yielded 51% of the desired compound after recrystallization from  $\text{CH}_2\text{Cl}_2$ / $\text{CH}_3\text{OH}$  (56.62 mg, 0.066 mmol). The last (red) fraction was identified as a cyano-substituted porphodimethene (**41**). m.p. 282 °C. –  $^1\text{H}$  NMR (500 MHz,  $\text{CDCl}_3$ ,  $\text{SiMe}_4$ ):  $\delta$  = 0.55 (18 H, m,  $\text{CH}_2\text{CH}_3$ ,  $2 \times \text{CH}_2\text{CH}_2\text{CH}_2\text{CH}_3$ ), 1.01 (m, 8 H,  $\text{CH}_2\text{CH}_2\text{CH}_2\text{CH}_3$ ), 1.52 (12 H, m,  $\text{CH}_2\text{CH}_3$ ), 2.30, 3.34 (16 H, m,  $\text{CH}_2\text{CH}_3$ ), 3.92 (m, 4 H,  $\text{CH}_2\text{CH}_2\text{CH}_2\text{CH}_3$ ), 7.53 (m, 4 H,  $\text{H}_{\text{Ph}}$ ), 7.60 (m, 2 H,  $\text{H}_{\text{Ph}}$ ), 7.85 (m, 4 H, br.,  $\text{H}_{\text{Ph}}$ ). – UV/Vis ( $\text{CH}_2\text{Cl}_2$ ):  $\lambda_{\text{max}}$  (lg  $\epsilon$ ) = 438 (4.90), 568 (3.88), 617 nm (3.71). – MS (80 eV);  $m/z$  (%) = 854 (100) [ $\text{M}^+$ ], 811 (11) [ $\text{M}^+ - \text{C}_3\text{H}_7$ ], 427 (17) [ $\text{M}^{2+}$ ]. – HRMS: calcd. for  $\text{C}_{56}\text{H}_{68}\text{N}_4\text{Ni}$  854.4797; found 854.4785.

**(5,10,15-Tributyl-2,3,7,8,12,13,17,18-octaethyl-20-phenylporphyrinato)nickel(II) (37):** For the preparation of this compound, **27** (100 mg, 0.13 mmol) was dissolved in THF (20 mL) at –100 °C and treated with BuLi (0.5 mmol) according to procedure A. Final purification on alumina (grade III), eluting with neat hexane, yielded three fractions. Product **37** was obtained in 54% yield after recrystallization from  $\text{CH}_2\text{Cl}_2$ /methanol (55 mg, 0.07 mmol). Starting material (11%) was recovered, together with a fraction containing two porphodimethenes (≈23%), one which was identified as **42** (see below). m.p. 268 °C. –  $^1\text{H}$  NMR (500 MHz,  $\text{CDCl}_3$ ,  $\text{SiMe}_4$ ):  $\delta$  = 0.59 (m, 9 H,  $\text{CH}_2\text{CH}_2\text{CH}_2\text{CH}_3$ ), 0.79, 0.86 (12 H, each t,  $\text{CH}_2\text{CH}_3$ ), 1.10 (12 H, m,  $\text{CH}_2\text{CH}_2\text{CH}_2\text{CH}_3$ ), 1.61, 1.78 (12 H, each t,  $\text{CH}_2\text{CH}_3$ ), 2.48 (m, 4 H,  $\text{CH}_2\text{CH}_3$ ), 3.40–3.67 (12 H, m,  $\text{CH}_2\text{CH}_3$ ), 3.91 (m, 2 H,  $\text{CH}_2\text{CH}_2\text{CH}_2\text{CH}_3$ ), 4.02 (m, 2 H,  $\text{CH}_2\text{CH}_2\text{CH}_2\text{CH}_3$ ), 7.34 (m, 4 H,  $\text{H}_{\text{Ph}}$ ), 7.55 (m, 1 H,  $\text{H}_{\text{Ph}}$ ), 8.55 (m, 2 H, br.,  $\text{H}_{\text{Ph}}$ ). – UV/Vis ( $\text{CH}_2\text{Cl}_2$ ):  $\lambda_{\text{max}}$  (lg  $\epsilon$ ) = 450 (4.94), 579 (4.32), 627 nm (4.44). – MS (80 eV);  $m/z$  (%) = 834 (100) [ $\text{M}^+$ ], 792 (17) [ $\text{M}^+ - \text{C}_3\text{H}_7$ ], 777 (59) [ $\text{M}^+ - \text{C}_4\text{H}_9$ ], 417 (16) [ $\text{M}^{2+}$ ]. – HRMS: calcd. for  $\text{C}_{54}\text{H}_{72}\text{N}_4\text{Ni}$  834.5153; found 834.51105.

**(5,15-Dibutyl-2,3,7,8,12,13,17,18-octaethyl-5,15-dihydro-10,20-diphenylporphyrinato)nickel(II) (40):** This compound was obtained as a side product during the synthesis of **36**. Purification of the apolar porphodimethene fraction required a second alumina column, eluting with neat hexane. The first (red) band was identified as the expected porphodimethene **40**, which was obtained as 23 mg (0.025 mmol, 19%) dark brown crystals. m.p. 225 °C. – <sup>1</sup>H NMR (500 MHz, CDCl<sub>3</sub>, SiMe<sub>4</sub>): δ = 0.47 (12 H, m, CH<sub>2</sub>CH<sub>3</sub>), 0.83 (16 H, CH<sub>2</sub>CH<sub>3</sub>; 2 × CH<sub>2</sub>CH<sub>2</sub>CH<sub>2</sub>CH<sub>3</sub>), 1.22–1.43 (16 H, m, 2 × CH<sub>2</sub>CH<sub>2</sub>CH<sub>2</sub>CH<sub>3</sub>, CH<sub>2</sub>CH<sub>3</sub>), 2.14 (m, 8 H, 4 × CH<sub>2</sub>CH<sub>3</sub>), 3.74 (m, 4 H, 2 × CH<sub>2</sub>CH<sub>2</sub>CH<sub>2</sub>CH<sub>3</sub>), 3.72 (m, 2 H, 5-, 15-H), 7.20–7.40 (m, 2 H, H<sub>Ph</sub>), 7.60 (m, 8 H, br, H<sub>Ph</sub>). – UV/Vis (CH<sub>2</sub>Cl<sub>2</sub>): λ<sub>max</sub> (lg ε) = 447 (4.61), 550 nm (3.73). – MS (80 eV); *m/z* (%) = 856 (60) [M<sup>+</sup>], 799 (100) [M<sup>+</sup> – C<sub>4</sub>H<sub>9</sub>], 742 (39) [M<sup>+</sup> – 2 × C<sub>4</sub>H<sub>9</sub>], 428 (9) [M<sup>2+</sup>].

**(5,15-Dibutyl-5-cyano-2,3,7,8,12,13,17,18-octaethyl-15-hydro-10,20-diphenylporphyrinato)nickel(II) (41):** The compound was obtained as a side product during the synthesis of **36**. Recrystallization from CH<sub>2</sub>Cl<sub>2</sub>/methanol gave 9 mg (0.011 mmol, 10%) dark brown crystals. m.p. 201 °C. – <sup>1</sup>H NMR (500 MHz, CDCl<sub>3</sub>, SiMe<sub>4</sub>): δ = 0.55 (12 H, m, CH<sub>2</sub>CH<sub>3</sub>), 0.93 (12 H, m, CH<sub>2</sub>CH<sub>2</sub>CH<sub>2</sub>CH<sub>3</sub>, 2 × CH<sub>2</sub>CH<sub>3</sub>), 1.12 (m, 4 H, CH<sub>2</sub>CH<sub>2</sub>CH<sub>2</sub>CH<sub>3</sub>), 1.29 (m, 6 H, 2 × CH<sub>2</sub>CH<sub>3</sub>), 1.45 (m, 4 H, CH<sub>2</sub>CH<sub>2</sub>CH<sub>2</sub>CH<sub>3</sub>), 1.65 (m, 4 H, CH<sub>2</sub>CH<sub>3</sub>), 1.81 (m, 2 H, CH<sub>2</sub>CH<sub>3</sub>), 2.00 (m, 2 H, CH<sub>2</sub>CH<sub>3</sub>), 2.10 (m, 4 H, CH<sub>2</sub>CH<sub>3</sub>), 2.26 (m, 4 H, CH<sub>2</sub>CH<sub>3</sub>), 2.61 (m, 2 H, 5-CH<sub>2</sub>CH<sub>2</sub>CH<sub>2</sub>CH<sub>3</sub>), 3.52 (m, 2 H, 15-CH<sub>2</sub>CH<sub>2</sub>CH<sub>2</sub>CH<sub>3</sub>), 3.69 (t, 1 H, <sup>3</sup>J = 7.2 Hz, 15-H), 7.29 (m, 4 H, H<sub>Ph</sub>), 7.40 (m, 4 H, H<sub>Ph</sub>), 7.60 (d, 2 H, H<sub>Ph</sub>). – UV/Vis (CH<sub>2</sub>Cl<sub>2</sub>): λ<sub>max</sub> (lg ε) = 450 (4.67), 551 nm (3.81). – MS (80 eV); *m/z* (%) = 881 (46) [M<sup>+</sup>], 854 (11) [M<sup>+</sup> – HCN], 824 (100) [M<sup>+</sup> – C<sub>4</sub>H<sub>9</sub>], 797 (16) [M<sup>+</sup> – C<sub>4</sub>H<sub>9</sub> – HCN], 441 (13) [M<sup>2+</sup>]. – HRMS: calcd. for C<sub>57</sub>H<sub>69</sub>N<sub>5</sub>Ni 881.4906; found 881.4979.

**(5,10,15-Tributyl-2,3,7,8,12,13,17,18-octaethyl-10,20-dihydro-20-phenylporphyrinato)nickel(II) (42):** This compound was obtained as a side product during the synthesis of **37**. Final purification of the porphodimethene fraction was by a second chromatographic column, eluting with *n*-hexane, and gave two fractions of which only the faster running one (red band) could be identified. Recrystallization from CH<sub>2</sub>Cl<sub>2</sub>/methanol gave 15 mg (0.018 mmol, 13.8%) dark brown crystals. m.p. 195 °C. – <sup>1</sup>H NMR (500 MHz, CDCl<sub>3</sub>, SiMe<sub>4</sub>): δ = 0.70–1.11 (27 H, m, CH<sub>2</sub>CH<sub>2</sub>CH<sub>2</sub>CH<sub>3</sub>, CH<sub>2</sub>CH<sub>3</sub>), 1.32–1.51 (12 H, m, 3 × CH<sub>2</sub>CH<sub>2</sub>CH<sub>2</sub>CH<sub>3</sub>), 1.81 (m, 6 H, CH<sub>2</sub>CH<sub>3</sub>), 2.30 (m, 4 H, CH<sub>2</sub>CH<sub>3</sub>), 2.42 (m, 4 H, CH<sub>2</sub>CH<sub>3</sub>), 2.60 (m, 8 H, CH<sub>2</sub>CH<sub>3</sub>), 2.83 (m, 2 H, CH<sub>2</sub>CH<sub>2</sub>CH<sub>2</sub>CH<sub>3</sub>), 2.92 (m, 4 H, CH<sub>2</sub>CH<sub>2</sub>CH<sub>2</sub>CH<sub>3</sub>), 3.71 (t, 1 H, <sup>3</sup>J = 7.2 Hz, 10-H), 5.22 (s, 1 H, 20-H), 7.20 (m, 1 H, H<sub>Ph</sub>), 7.40 (m, 2 H, H<sub>Ph</sub>), 8.33 (d, 2 H, H<sub>Ph</sub>). – UV/Vis (CH<sub>2</sub>Cl<sub>2</sub>): λ<sub>max</sub> (lg ε) = 450 (4.67), 551 nm (3.81). – MS (80 eV); *m/z* (%) = 836 (12) [M<sup>+</sup>], 779 (48) [M<sup>+</sup> – C<sub>4</sub>H<sub>9</sub>], 418 (3) [M<sup>2+</sup>]. – HRMS: calcd. for C<sub>54</sub>H<sub>74</sub>N<sub>4</sub>Ni 836.5267; found 836.5225.

**(2,3,7,8,12,13,17,18-Octaethyl-5,15-dihydro-5,15-diphenylporphyrin (44):** This compound was obtained as a new side product from the synthesis of 2,3,7,8,12,13,17,18-octaethyl-5,15-diphenylporphyrin (**20**) following the procedure given by Ogoshi et al.<sup>[26]</sup> For oxidation, four equivalents of DDQ were used. Chromatography of the reaction mixture on alumina with dichloromethane/*n*-hexane (1:6, v/v) gave four products. The second band contained the desired porphyrin **20** as the major product (32%), followed by two minor products identified as the monophenylated (**10**, 2.5%) and 5,10-diphenylated (**14**, 2.5%) porphyrins. The title porphodimethene eluted as the most apolar compound (red band). Recrystallization from CH<sub>2</sub>Cl<sub>2</sub>/methanol yielded 62 mg (0.090 mmol, 5%). m.p. 204

°C. – <sup>1</sup>H NMR (500 MHz, CDCl<sub>3</sub>, SiMe<sub>4</sub>): δ = 1.07, 1.20 (24 H, each t, <sup>3</sup>J = 7.6 Hz, CH<sub>2</sub>CH<sub>3</sub>), 1.55 (s, 2 H, br, NH), 2.60 (16 H, q, <sup>3</sup>J = 7.8 Hz, CH<sub>2</sub>CH<sub>3</sub>), 5.39 (s, 2 H, 5-, 15-H), 6.63 (s, 2 H, 10-, 20-H), 7.20 (m, 6 H, H<sub>Ph</sub>), 7.63 (d, 4 H, <sup>3</sup>J = 4 Hz, H<sub>Ph</sub>). – UV/Vis (CH<sub>2</sub>Cl<sub>2</sub>): λ<sub>max</sub> (lg ε) = 428 nm (4.95). – MS (80 eV); *m/z* (%) = 688 (100) [M<sup>+</sup>], 673 (3) [M<sup>+</sup> – CH<sub>3</sub>], 659 (5) [M<sup>+</sup> – C<sub>2</sub>H<sub>5</sub>], 611 (16) [M<sup>+</sup> – C<sub>6</sub>H<sub>5</sub>], 344 (11) [M<sup>2+</sup>]. – HRMS: calcd. for C<sub>48</sub>H<sub>56</sub>N<sub>4</sub> 688.4505; found 688.4552.

**(5-Butyl-5-cyano-2,3,7,8,12,13,17,18-octaethyl-10,20-diphenylporphyrinato)nickel(II) (45):** This compound was prepared from **22**, following procedure A with BuLi. However, the addition of water was omitted here. The porphyrin **26** (32%), an unknown porphodimethene, starting material, and compound **45** were obtained. Final purification of the fraction containing both the starting material **22** and compound **45** was achieved with a second chromatographic column of alumina, eluting with dichloromethane/*n*-hexane (1:12, v/v). The slower running (green) band was identified after crystallization from CH<sub>2</sub>Cl<sub>2</sub>/methanol as the cyano side product. Analytical HPLC (*n*-hexane/dichloromethane, 7:3) confirmed the purity of the cyano compound. Yield: 21 mg (0.025 mmol, 23%). m.p. 228 °C. – <sup>1</sup>H NMR (500 MHz, CDCl<sub>3</sub>, SiMe<sub>4</sub>): δ = 0.48, 0.60 (12 H, each t, <sup>3</sup>J = 7.5 Hz, CH<sub>2</sub>CH<sub>3</sub>), 0.83 (t, 3 H, <sup>3</sup>J = 7.3 Hz, CH<sub>2</sub>CH<sub>2</sub>CH<sub>2</sub>CH<sub>3</sub>), 1.40 (m, 4 H, CH<sub>2</sub>CH<sub>2</sub>CH<sub>2</sub>CH<sub>3</sub>), 1.49 (12 H, t, <sup>3</sup>J = 7.5 Hz, CH<sub>2</sub>CH<sub>3</sub>), 2.25, 2.42, 3.30, 3.69 (16 H, each q, <sup>3</sup>J = 7.5 Hz, CH<sub>2</sub>CH<sub>3</sub>), 4.06 (m, 2 H, CH<sub>2</sub>CH<sub>2</sub>CH<sub>2</sub>CH<sub>3</sub>), 7.52 (m, 4 H, H<sub>Ph</sub>), 7.62 (t, 2 H, <sup>3</sup>J = 7 Hz, H<sub>Ph</sub>), 7.91 (s, 4 H, br., <sup>3</sup>J = 7.5 Hz, H<sub>Ph</sub>). – <sup>13</sup>C NMR (CDCl<sub>3</sub>) δ = 14.02 (CH<sub>3</sub>-butyl), 17.00 (CH<sub>3</sub>-ethyl), 17.10 (CH<sub>3</sub>-ethyl), 120.00 (CH<sub>2</sub>-ethyl), 20.03, 20.20 (CH<sub>2</sub>-ethyl), 21.02 (CH<sub>2</sub>-ethyl), 29.98 (CH<sub>2</sub>-butyl), 32.01 (CH<sub>2</sub>-butyl), 37.18 (CH<sub>2</sub>-butyl), 119.97, 120.05, 122.00 (5-, 10-, 15-, 20-C), 126.04, 128.02, 132.07, 138.06 (C<sub>Ph</sub>), 139.09, 142.10 (1-, 4-, 6-, 9-, 11-, 14-, 16-, 19-), 142.41 (CN), 144.46, 146.02, 146.73, 148.37 (2-, 3-, 7-, 8-, 12-, 13-, 17-, 18-C). – UV/Vis (CH<sub>2</sub>Cl<sub>2</sub>): λ<sub>max</sub> (lg ε) = 436 (4.82), 633 nm (3.70). – MS (80 eV); *m/z* (%) = 823 (100) [M<sup>+</sup>], 780 (15) [M<sup>+</sup> – C<sub>3</sub>H<sub>7</sub>], 412 (14) [M<sup>2+</sup>]. – HRMS: calcd. for C<sub>53</sub>H<sub>59</sub>N<sub>5</sub>Ni 823.4124; found 823.4137.

**2,3,7,8,12,13,17,18-Octaethyl-5-phenoxyphyrin (46):** During attempts to prepare 2,3,7,8,12,13,17,18-octaethyl-5-phenylporphyrin **10** following procedure B we observed that the use of opened, older stock solutions of PhLi (Aldrich, about 6 months after opening) led to a decrease in the yield, from 98% obtained with freshly opened bottles of PhLi to 63%. Column chromatography of the reaction product on alumina with dichloromethane/hexane (1:10, v/v) yielded **46** as a second, slower running fraction. Yield 37 mg (0.06 mmol, 35%) of purple crystals after crystallization from CH<sub>2</sub>Cl<sub>2</sub>/methanol. m.p. 223 °C. – <sup>1</sup>H NMR (500 MHz, CDCl<sub>3</sub>, SiMe<sub>4</sub>): δ = –3.31 (s, 2 H, br., NH), 1.73, 1.78, 1.89 (24 H, each t, <sup>3</sup>J = 7.5 Hz, CH<sub>2</sub>CH<sub>3</sub>), 3.75 (m, 4 H, CH<sub>2</sub>CH<sub>3</sub>), 4.0 (12 H, m, CH<sub>2</sub>CH<sub>3</sub>), 6.69 (d, 2 H, <sup>3</sup>J = 4.5 Hz, H<sub>Ph</sub>), 6.90 (t, 1 H, <sup>3</sup>J = 7.2 Hz, H<sub>Ph</sub>), 7.12 (t, 2 H, <sup>3</sup>J = 7.6 Hz, H<sub>Ph</sub>), 9.82 (s, 1 H, 15-H), 10.01 (s, 2 H, 10-, 20-H). – <sup>13</sup>C NMR (125 MHz, CDCl<sub>3</sub>): δ = 14.10, 16.78, 17.25, 18.48, 19.63, 19.73, 19.76, 20.62, 21.61, 24.10, 29.72 (CH<sub>2</sub>CH<sub>3</sub>, CH<sub>2</sub>CH<sub>3</sub>), 96.36, 96.83, 115.16, 129.56 (C<sub>Ph</sub>), 116.18, 118.91, 121.41, 123.58 (5-, 10-, 15-, 20-C), 139.92, 140.74, 151.00, 142.14, 142.31, 142.58, 143.02, 143.34, 145.71 (1-, 2-, 3-, 4-, 6-, 7-, 8-, 9-, 11-, 12-, 13-, 14-, 16-, 17-, 18-, 19-C). – UV/Vis (CH<sub>2</sub>Cl<sub>2</sub>): λ<sub>max</sub> (lg ε) = 405 (5.56), 502 (4.54), 536 (4.17), 572 (4.55), 625 nm (3.52). – MS (80 eV); *m/z* (%) = 626 (100) [M<sup>+</sup>], 611 (5) [M<sup>+</sup> – CH<sub>3</sub>], 549 (6) [M<sup>+</sup> – C<sub>6</sub>H<sub>5</sub>], 313 (17) [M<sup>2+</sup>]. – HRMS: calcd. for C<sub>42</sub>H<sub>50</sub>N<sub>4</sub>NiO 626.3985; found 626.3984.

**2,3,7,8,12,13,17,18-Octaethyl-5-phenoxy-10,15,20-triphenylporphyrin (47):** A solution of **25** (100 mg, 0.15 mmol) was treated

with PhLi according to general procedure B, but using older, opened stock solutions of PhLi. Column chromatography on alumina, eluting with dichloromethane/hexane (1:16, v/v), gave a ma-

jor (green) band of recovered starting material (66%) and a minor, slower running band of **47**. Yield 27 mg (0.03 mmol, 20%) of purple crystals. m.p. 245 °C. – <sup>1</sup>H NMR (500 MHz, CDCl<sub>3</sub>, SiMe<sub>4</sub>): δ =

Table 3. Summary of crystal data, data collection, and refinement for the crystal structure determinations

Compound	11	14	16	18	23
chemical formula	C <sub>38</sub> H <sub>50</sub> N <sub>4</sub> Ni·1/2C <sub>5</sub> H <sub>5</sub> N	C <sub>48</sub> H <sub>54</sub> N <sub>4</sub> ·CH <sub>2</sub> Cl <sub>2</sub>	C <sub>48</sub> H <sub>52</sub> N <sub>4</sub> Ni·CH <sub>2</sub> Cl <sub>2</sub>	C <sub>49</sub> H <sub>56</sub> N <sub>4</sub> OZn	C <sub>46</sub> H <sub>56</sub> N <sub>4</sub> Ni·H <sub>2</sub> O
mol. mass	687.12	771.88	828.57	782.35	741.67
crystallization	CH <sub>2</sub> Cl <sub>2</sub> /CH <sub>3</sub> OH+pyr	CH <sub>2</sub> Cl <sub>2</sub> /CH <sub>3</sub> OH	CH <sub>2</sub> Cl <sub>2</sub> /CH <sub>3</sub> OH	CH <sub>2</sub> Cl <sub>2</sub> /CH <sub>3</sub> OH	CH <sub>2</sub> Cl <sub>2</sub> /CH <sub>3</sub> OH(wet)
color, habit	red parallel epiped	blue plate	blue parallel epiped	red block	red plate
crystal size [mm]	1 × 0.3 × 0.3	0.2 × 0.15 × 0.04	0.62 × 0.1 × 0.1	0.10 × 0.08 × 0.08	0.24 × 0.24 × 0.02
lattice type	triclinic	monoclinic	monoclinic	triclinic	triclinic
space group	<i>P</i> $\bar{1}$	<i>C</i> 2/ <i>c</i>	<i>C</i> 2/ <i>c</i>	<i>P</i> $\bar{1}$	<i>P</i> $\bar{1}$
<i>a</i> [Å]	12.015(5)	35.258(15)	34.614(15)	7.572(3)	11.3144(4)
<i>b</i> [Å]	13.059(7)	10.985(3)	11.545(5)	14.701(5)	13.3809(4)
<i>c</i> [Å]	13.987(6)	24.168(11)	23.934(4)	19.298(6)	14.9154(5)
$\alpha$ [°]	69.47(4)			72.33(3)	93.927(1)
$\beta$ [°]	66.49(4)	119.12(3)	120.15(3)	88.63(3)	110.532(1)
$\gamma$ [°]	73.26(4)			80.77(3)	107.683(1)
<i>V</i> [Å <sup>3</sup> ]	1856.5(15)	8409(6)	8271(5)	2019.4(11)	1975.64(11)
<i>Z</i>	2	8	8	2	2
<i>d</i> <sub>calcd.</sub> [Mg m <sup>−3</sup> ]	1.229	1.219	1.331	1.287	1.247
$\mu$ [mm <sup>−1</sup> ]	1.012	1.676	2.166	1.162	0.531
<i>T</i> <sub>max</sub> , <i>T</i> <sub>min</sub>	0.75, 0.43	0.94, 0.73	0.81, 0.35	0.91, 0.89	0.99, 0.88
$\theta$ <sub>max</sub> [°]	56.45	56.48	56.51	56.45	31.53
<i>T</i> [K]	123	130	130	130	90
collec. reflections	4814	6035	5940	5816	28375
indep. reflections	4566	5573	5488	5333	12453
reflections with <i>F</i> > 4.0σ( <i>F</i> )	4137	3618	4173	4545	8109
<i>R</i> <sub>int</sub>	0.0282	0.0818	0.0696	0.0367	0.0475
no. of parameters	459	420	514	505	473
$\Delta/\rho$ <sub>max</sub> [e Å <sup>−3</sup> ]	0.846	0.608	0.525	0.459	1.271
<i>R</i> 1 [ <i>F</i> > 4.0σ( <i>F</i> )]	0.0660	0.0666	0.0574	0.0382	0.0515
<i>wR</i> 2 [ <i>F</i> > 4.0σ( <i>F</i> )]	0.1870	0.1721	0.1333	0.0911	0.1221
<i>R</i> 1 (all data)	0.0707	0.1122	0.0811	0.0487	0.0907
<i>wR</i> 2 (all data)	0.1929	0.2140	0.1594	0.0984	0.1363

Table 4. Summary of crystal data, data collection, and refinement for the crystal structure determinations

Compound	24	26	45	48
chemical formula	C <sub>54</sub> H <sub>58</sub> N <sub>4</sub>	C <sub>52</sub> H <sub>60</sub> N <sub>4</sub> Ni	C <sub>53</sub> H <sub>59</sub> N <sub>5</sub> Ni	C <sub>60</sub> H <sub>60</sub> N <sub>4</sub> NiO·CH <sub>2</sub> Cl <sub>2</sub>
mol. mass	763.04	799.75	824.76	996.76
crystallization	CH <sub>2</sub> Cl <sub>2</sub> / <i>n</i> -hexane	CH <sub>2</sub> Cl <sub>2</sub> /CH <sub>3</sub> OH	CH <sub>2</sub> Cl <sub>2</sub> /CH <sub>3</sub> OH	CH <sub>2</sub> Cl <sub>2</sub> /CH <sub>3</sub> OH
color, habit	green rhombus	brown plate	green-black block	red block
crystal size [mm]	0.24 × 0.16 × 0.12	0.6 × 0.4 × 0.1	0.24 × 0.24 × 0.08	0.3 × 0.15 × 0.15
lattice type	triclinic	monoclinic	triclinic	triclinic
space group	<i>P</i> $\bar{1}$	<i>P</i> 2 <sub>1</sub>	<i>P</i> $\bar{1}$	<i>P</i> $\bar{1}$
<i>a</i> [Å]	12.653(3)	12.910(4)	12.328(3)	13.308(9)
<i>b</i> [Å]	14.104(4)	25.857(6)	13.783(3)	13.912(8)
<i>c</i> [Å]	14.231(4)	13.556(3)	14.058(3)	14.519(7)
$\alpha$ [°]	79.89(2)		89.88(2)	72.82(4)
$\beta$ [°]	75.63(2)	107.16(2)	70.97(2)	77.78(5)
$\gamma$ [°]	63.49(2)		74.56(2)	80.41(5)
<i>V</i> [Å <sup>3</sup> ]	2195.5(10)	4323.7(13)	2167.3(9)	2588(3)
<i>Z</i>	2	4 (2 indep. mol.)	2	2
<i>d</i> <sub>calcd.</sub> [Mg m <sup>−3</sup> ]	1.154	1.229	1.264	1.279
$\mu$ [mm <sup>−1</sup> ]	0.509	0.941	0.962	1.836
<i>T</i> <sub>max</sub> , <i>T</i> <sub>min</sub>	0.94, 0.89	0.91, 0.60	0.93, 0.80	0.77, 0.61
$\theta$ <sub>max</sub> [°]	56.44	56.44	56.45	56.34
<i>T</i> [K]	123	124	130	130
collec. reflections	6135	6015	6051	7156
indep. reflections	5819	5704	5728	6812
reflections with <i>F</i> > 4.0σ( <i>F</i> )	4156	4938	4949	5103
<i>R</i> <sub>int</sub>	0.0374	0.0322	0.0604	0.085
no. of parameters	531	1051	541	631
$\Delta/\rho$ <sub>max</sub> [e Å <sup>−3</sup> ]	0.413	0.922	0.707	1.151
<i>R</i> 1 [ <i>F</i> > 4.0σ( <i>F</i> )]	0.0532	0.0629	0.0589	0.0773
<i>wR</i> 2 [ <i>F</i> > 4.0σ( <i>F</i> )]	0.1229	0.1528	0.1499	0.1977
<i>R</i> 1 (all data)	0.0838	0.0813	0.0684	0.1030
<i>wR</i> 2 (all data)	0.1398	0.1739	0.1563	0.2180



0.40 (12 H, t,  $^3J = 7.5$  Hz,  $4 \times \text{CH}_2\text{CH}_3$ ), 0.90 (t, 6 H,  $^3J = 7.5$  Hz,  $2 \times \text{CH}_2\text{CH}_3$ ), 1.40 (t, 6 H,  $^3J = 7.5$  Hz,  $2 \times \text{CH}_2\text{CH}_3$ ), 2.19 (12 H, m,  $\text{CH}_2\text{CH}_3$ ), 3.26 (m, 4 H, 2-, 3-, 7-, 8- $\text{CH}_2\text{CH}_3$ ), 7.35 (m, 2 H,  $\text{H}_{\text{OPh}}$ ), 7.52 (m, 2 H,  $\text{H}_{\text{OPh}}$ ), 7.63 (m, 9 H,  $\text{H}_{\text{Ph}}$ ), 8.29 (m, 6 H,  $\text{H}_{\text{Ph}}$ ). – UV/Vis ( $\text{CH}_2\text{Cl}_2$ ):  $\lambda_{\text{max}}$  (lg  $\epsilon$ ) 446 (5.09), 528 (3.08), 574 (3.25), 629 nm (2.40). – MS (80 eV);  $m/z$  (%) = 854 (100) [ $\text{M}^+$ ], 427 (22) [ $\text{M}^{2+}$ ]. – HRMS: calcd. for  $\text{C}_{60}\text{H}_{62}\text{N}_4\text{NiO}$  854.49236; found 854.4924.

**(2,3,7,8,12,13,17,18-Octaethyl-5-phenoxy-10,15,20-triphenylporphyrinato)nickel(II) (48):** The nickel(II) complex was prepared using the standard acetate procedure, with **47** (200 mg, 0.23 mmol) as starting material. After purification by column chromatography on alumina, eluting with dichloromethane/hexane (1:4, v/v), 180 mg (0.20 mmol, 87%) of title compound were obtained as purple crystals from  $\text{CH}_2\text{Cl}_2$ /methanol. m.p. 256 °C. –  $^1\text{H}$  NMR (500 MHz,  $\text{CDCl}_3$ ,  $\text{SiMe}_4$ ):  $\delta$  = 0.50 (12 H, t,  $^3J = 7.5$  Hz,  $4 \times \text{CH}_2\text{CH}_3$ ), 1.26 (t, 6 H,  $^3J = 7.5$  Hz,  $2 \times \text{CH}_2\text{CH}_3$ ), 1.31 (t, 6 H,  $2 \times \text{CH}_2\text{CH}_3$ ), 2.22 (m, 8 H,  $\text{CH}_2\text{CH}_3$ ), 3.13 (m, 8 H,  $4 \times \text{CH}_2\text{CH}_3$ ), 6.61 (m, 1 H,  $\text{H}_{\text{OPh}}$ ), 6.99 (m, 2 H,  $\text{H}_{\text{OPh}}$ ), 7.21 (m, 2 H,  $\text{H}_{\text{OPh}}$ ), 7.52 (m, 9 H,  $\text{H}_{\text{Ph}}$ ), 8.07 (m, 6 H,  $\text{H}_{\text{Ph}}$ ). – UV/Vis ( $\text{CH}_2\text{Cl}_2$ ):  $\lambda_{\text{max}}$  (lg  $\epsilon$ ) 448 (4.80), 581 (3.78), 637 nm (3.41). – MS (80 eV);  $m/z$  (%) = 910 (100) [ $\text{M}^+$ ], 833 (4) [ $\text{M}^+ - \text{C}_5\text{H}_6$ ], 455 (26) [ $\text{M}^{2+}$ ]. – HRMS: calcd. for  $\text{C}_{60}\text{H}_{60}\text{N}_4\text{ONi}$  910.4121; found 910.4102.

**X-ray Crystallographic Studies:**<sup>[39]</sup> Crystals were selected and mounted as described by Hope.<sup>[40]</sup> Data for **11**, **14**, **16**, **18**, **24**, **26**, **45**, and **48** were collected with a Siemens P4 rotating anode instrument at 130 K using Ni-filtered  $\text{Cu-K}\alpha$  radiation ( $\lambda = 1.54178$  Å). During data collection, two standard reflections were measured every 198 reflections and showed only statistical variation of the intensities (<1%). Data for **23** were collected with a Siemens SMART instrument, complete with 3-circle goniometer and CCD detector utilizing  $\text{Mo-K}\alpha$  radiation ( $\lambda = 0.71073$  Å). The intensities were corrected for Lorentz and polarization effects. For all structures, an absorption correction was applied using the program XABS2,<sup>[41a]</sup> while extinction effects were disregarded. For **23**, an absorption correction was applied using the program SADABS.<sup>[41b]</sup> The free base structures were solved by Direct Methods,<sup>[42a]</sup> missing atoms and solvent molecules were located in subsequent Fourier difference maps; structure of the metal complexes were solved by Patterson syntheses.<sup>[42a]</sup> Refinements were carried out by full-matrix, least-squares on  $|F^2|$  using the program SHELXL-97.<sup>[42b]</sup> Hydrogen atoms were included at calculated positions using a riding model with  $\text{C-H} = 0.96$  Å and  $\text{N-H} = 0.90$  Å; unless otherwise stated, all non-hydrogen atoms were refined with anisotropic thermal parameters. Details for the crystal data, data collection, and refinement are given in Table 3 and Table 4.

Refinement details for **11**: One ethyl group (C171, C172) was disordered and refined with two split positions of equal occupancy. A pyridine of solvation was located in a special position and refined with half occupancy. – **27**: Disorder in some ethyl side chains. C3A and C38B were refined as disordered over two split positions with equal occupancy. C37B was refined as disordered over two split positions with occupancies of 0.35 and 0.65, respectively. The absolute structure was determined by refinement of the Flack parameter<sup>[43]</sup> which refined to 0.05(6). – **53**: A dichloromethane of solvation was refined with a common free variable for the occupancy which refined to 0.65.

## Acknowledgments

This work was generously supported by grants from the Deutsche Forschungsgemeinschaft (Se543/2-5/5-1 and Heisenberg fellowship

Se543/3-2) and the Fonds der Chemischen Industrie. We are indebted to the UC Davis crystallographic facility (M. M. Olmstead, director) and Schering AG (Berlin) for their support.

- [1] [1a] S. Hanessian, G. McNaughton-Smith, H. G. Lomhart, W. D. Lubell, *Tetrahedron* **1997**, *53*, 12789–12854. G. D. Glick, *Biopolymers* **1998**, *48*, 83–96. R. W. Hoffmann, *Angew. Chem. Int. Ed.* **2000**, *39*, 2054–2070. J. A. Robinson, *Synlett* **2000**, 429–441. – [1b] K. M. Barkigia, L. Chantranupong, K. M. Smith, J. Fajer, *J. Am. Chem. Soc.* **1988**, *110*, 7566–7567. – [1c] M. O. Senge, *J. Photochem. Photobiol. B: Biol.* **1992**, *16*, 3–36. M. Ravikanth, T. K. Chandrashekar, *Struct. Bonding* **1995**, *82*, 105–188.
- [2] M. O. Senge, in: *The Porphyrin Handbook* (Eds.: K. M. Kadish, K. M. Smith, R. Guilard), Academic Press, San Diego, CA, **2000**, Vol. 1, p. 239–347.
- [3] [3a] D. E. Tronrud, M. F. Schmid, B. W. Matthews, *J. Mol. Biol.* **1986**, *188*, 443–454. S. M. Prince, M. Z. Papiz, A. A. Freer, G. McDermott, A. M. Hawthornwaite-Lawless, R. J. Cogdell, N. W. Isaacs, *J. Mol. Biol.* **1997**, *268*, 412–423. – [3b] J. Deisenhofer, O. Epp, K. Mikki, R. Huber, H. Michel, *Nature* **1985**, *318*, 618–624. M. Plato, K. Möbius, M. E. Michel-Beyerle, M. Bixon, J. Jortner, *J. Am. Chem. Soc.* **1988**, *110*, 7279–7285. J. R. Norris, D. E. Budil, P. Gast, C.-H. Chang, O. El-Kabbani, M. Schiffer, *Proc. Natl. Acad. Sci. USA* **1989**, *86*, 4335–4339. C. Kirmayer, D. Holten, *Proc. Natl. Acad. Sci. USA* **1990**, *87*, 3552–3556. A. J. Chirino, E. J. Lous, M. Huber, J. P. Allen, C. C. Schenck, M. L. Paddock, G. Feher, D. C. Rees, *Biochemistry* **1994**, *33*, 4584–4593. J. Koepke, X. Hu, C. Muenke, K. Schulten, H. Michel, *Structure* **1996**, *4*, 581–597. – [3c] G. R. Moore, G. W. Pettigrew, *Cytochromes c*. Springer-Verlag, Berlin, **1990**. [3d] T. L. Poulos, in: *The Porphyrin Handbook* (Eds.: K. M. Kadish, K. M. Smith, R. Guilard), Academic Press, San Diego, CA, **2000**, Vol. 4, p. 189–218.
- [4] A. M. Berghuis, G. D. Brayer, *J. Mol. Biol.* **1992**, *223*, 959–976. I. Schlichting, J. Berendzen, G. N. Phillips Jr., R. M. Sweet, *Nature* **1994**, *371*, 808–812. S. Othman, J. Fitch, M. A. Cusanowich, A. Desbois, *Biochemistry* **1997**, *36*, 5499–5508. I. Schlichting, J. Berendzen, K. Chu, A. M. Stock, S. A. Maves, D. E. Benson, R. M. Sweet, D. Ringe, G. A. Petsko, S. G. Sligar, *Science* **2000**, *287*, 1615–1622.
- [5] For a complete discussion of the various biological examples and structural and spectroscopic evidence for the conformational control of biological reactions see references [1c, 2, 3d].
- [6] M. B. Hursthouse, S. Neidle, *J. Chem. Soc., Chem. Commun.* **1972**, 449–450. J.-H. Fuhrhop, L. Witte, W. S. Sheldrick, *Liebigs Ann. Chem.* **1976**, 1537–1559.
- [7] [7a] D. Dolphin, *J. Heterocycl. Chem.* **1970**, *7*, 275–283. J. A. Shelnutt, C. J. Medforth, M. D. Berber, K. M. Barkigia, K. M. Smith, *J. Am. Chem. Soc.* **1991**, *113*, 4077–4087. L. D. Sparks, C. J. Medforth, M.-S. Park, J. R. Chamberlain, M. R. Ondrias, M. O. Senge, K. M. Smith, J. A. Shelnutt, *J. Am. Chem. Soc.* **1993**, *115*, 581–592. – [7b] L. D. Sparks, K. K. Anderson, C. J. Medforth, K. M. Smith, J. A. Shelnutt, *Inorg. Chem.* **1994**, *32*, 2297–2302. – [7c] M. O. Senge, T. P. Forsyth, L. T. Nguyen, K. M. Smith, *Angew. Chem. Int. Ed. Engl.* **1994**, *33*, 2485–2487. – [7d] X. Zhou, M. K. Tse, T. S. M. Wan, K. S. Chan, *J. Org. Chem.* **1996**, *61*, 3590–3593. – [7e] K. M. Barkigia, M. D. Berber, J. Fajer, C. J. Medforth, M. W. Renner, K. M. Smith, *J. Am. Chem. Soc.* **1990**, *112*, 8851–8857. – [7f] M. O. Senge, C. J. Medforth, L. D. Sparks, J. A. Shelnutt, K. M. Smith, *Inorg. Chem.* **1993**, *32*, 1716–1723. – [7g] K. M. Barkigia, M. W. Renner, L. R. Furenli, C. J. Medforth, K. M. Smith, J. Fajer, *J. Am. Chem. Soc.* **1993**, *115*, 3627–3635.
- [8] [8a] S. Tsuchiya, *Chem. Phys. Lett.* **1990**, *169*, 608–610. C. J. Medforth, K. M. Smith, *Tetrahedron Lett.* **1990**, *31*, 5583–5586. J. Takeda, M. Sato, *Chem. Lett.* **1995**, 939–940; 971–972. K. Perić, J.-M. Barbe, P. Cocolios, R. Guilard, *Bull. Soc. Chim. Fr.* **1996**, *113*, 697–702. N. Ono, H. Miyagawa, T. Ueta, T. Ogawa, H. Tani, *J. Chem. Soc., Perkin Trans. 1* **1998**, 1595–1601. C.-J. Liu, W.-Y. Yu, S.-M. Peng, T. C. W. Mak, C.-M. Che, *J. Chem. Soc., Dalton Trans.* **1998**, 1805–1812. – [8b] C. J. Medforth, M. O. Senge, K. M. Smith, L. D. Sparks, J. A. Shelnutt, *J. Am. Chem. Soc.* **1992**, *114*, 9859–9869. – [8c] M. O. Senge, *Z. Naturforsch., Teil B* **1999**, *54*, 821–824.
- [9] [9a] W. Kalisch, M. O. Senge, *Angew. Chem. Int. Ed.* **1998**, *37*, 1107–1109. M. O. Senge, W. W. Kalisch, I. Bischoff, *Chem.*



- Eur. J.* **2000**, *6*, 2721–2738. – [9b] M. O. Senge, M. W. Renner, W. W. Kalisch, J. Fajer, *J. Chem. Soc., Dalton Trans.* **2000**, 381–385.
- [10] D. Dolphin, T. D. Traylor, L. Y. Xie, *Acc. Chem. Res.* **1997**, *30*, 251–259. B. Meunier, A. Robert, G. Pratviel, J. Bernadou, in: *The Porphyrin Handbook* (Eds.: K. M. Kadish, K. M. Smith, R. Guilard), Academic Press, San Diego, CA, **2000**, Vol. 4, p. 119–187.
- [11] [11a] T. Ema, M. O. Senge, N. Y. Nelson, H. Ogoshi, K. M. Smith, *Angew. Chem. Int. Ed. Engl.* **1994**, *33*, 1879–1881. M. O. Senge, T. Ema, K. M. Smith, *Chem. Commun.* **1995**, 733–734. M. Mazzanti, J.-C. Marchon, M. Shang, W. R. Scheidt, S. Jia, J. A. Shelnutt, *J. Am. Chem. Soc.* **1997**, *119*, 12400–12401. – [11b] For a complete discussion of highly substituted, nonplanar porphyrins see ref. [2].
- [12] J. S. Lindsey, in: *The Porphyrin Handbook* (Eds.: K. M. Kadish, K. M. Smith, R. Guilard), Academic Press, San Diego, CA, **2000**, Vol. 1, p. 45–118.
- [13] W. R. Scheidt, Y.-J. Lee, *Struct. Bonding* **1987**, *64*, 1–70.
- [14] J. A. Shelnutt, in: *The Porphyrin Handbook* (Eds.: K. M. Kadish, K. M. Smith, R. Guilard), Academic Press, San Diego, CA, **2000**, Vol. 7, p. 167–223.
- [15] L.-C. Gong, D. Dolphin, *Can. J. Chem.* **1985**, *63*, 406–411. S. Banfi, A. Manfredi, G. Pozzi, S. Quici, A. Trebicka, *Gazz. Chim. Ital.* **1996**, *126*, 179–185. Y. Furusho, T. Kimura, Y. Mizuno, T. Aida, *J. Am. Chem. Soc.* **1997**, *119*, 5267–5268. K. M. Shea, L. Jaquinod, R. G. Khoury, K. M. Smith, *Chem. Commun.* **1998**, 759–760. M. O. Senge, V. Gerstung, K. Ruhlandt-Senge, S. Runge, I. Lehmann, *J. Chem. Soc., Dalton Trans.* **1998**, 4187–4199.
- [16] [16a] L.-C. Gong, D. Dolphin, *Can. J. Chem.* **1985**, *63*, 401–405. J. Takeda, M. Sato, *Chem. Lett.* **1994**, 2233–2236. M. O. Senge, W. W. Kalisch, S. Runge, *Tetrahedron* **1998**, *54*, 3781–3798. – [16b] M. O. Senge, W. W. Kalisch, *Inorg. Chem.* **1997**, *36*, 6103–6116.
- [17] M. O. Senge, C. J. Medforth, T. P. Forsyth, D. A. Lee, M. M. Olmstead, W. Jentzen, R. K. Pandey, J. A. Shelnutt, K. M. Smith, *Inorg. Chem.* **1997**, *36*, 1149–1163.
- [18] [18a] Total syntheses are limited with regard to the substituents that can be introduced at each step and have been studied only for  $\beta$ -unsubstituted porphyrins see ref. [18b]. – Mixed condensations, besides being aesthetically unappealing, require appropriate polarity differences between the porphyrins obtained to allow chromatographic separation. [18b] D. M. Wallace, S. H. Leung, M. O. Senge, K. M. Smith, *J. Org. Chem.* **1993**, *58*, 7245–7257. C.-H. Lee, F. Li, K. Iwamoto, J. Dadok, A. A. Bothner-By, J. S. Lindsey, *Tetrahedron* **1995**, *51*, 11645–11672. – [18c] Recently, Lindsey and co-workers published a report on using dipyrromethanes for the synthesis of ABCD-porphyrins without  $\beta$ -substituents. P. D. Rao, S. Dhanlekshmi, B. J. Littler, J. S. Lindsey, *J. Org. Chem.* **2000**, *65*, 7323–7344.
- [19] [19a] M. O. Senge, X. Feng, *Tetrahedron Lett.* **1999**, *40*, 4165–4168; M. O. Senge, X. Feng, *Perkin Trans. 1* **2000**, 3615–3621. – [19b] X. Feng, M. O. Senge, *Tetrahedron* **2000**, *56*, 587–590.
- [20] For related studies on the reactivity of other tetrapyrroles with LiR see: [20a] B. Krattinger, H. J. Callot, *Tetrahedron Lett.* **1996**, *37*, 7699–7702; B. Krattinger, H. J. Callot, **1998**, *39*, 1165–1168; B. Krattinger, H. J. Callot, *Eur. J. Org. Chem.* **1999**, 1857–1867. – [20b] L. Bonomo, E. Solari, R. Scopelliti, C. Floriani, N. Re, *J. Am. Chem. Soc.* **2000**, *122*, 5312–5326. J.-i. Setsune, T. Yazawa, H. Ogoshi, Z.-i. Yoshida, *J. Chem. Soc., Perkin Trans. 1* **1980**, 1641–1645.
- [21] K. Ziegler, H. Zeiser, *Ber. Dtsch. Chem. Ges.* **1930**, *63*, 1847–1851.
- [22] M. O. Senge, in: *The Porphyrin Handbook* (Eds.: K. M. Kadish, K. M. Smith, R. Guilard), Academic Press, San Diego, CA, **1999**, Vol. 10, p. 1–218.
- [23] A few syntheses of  $A_2$ -porphyrins with mixed condensations under which scrambling was suppressed have been described.
- [27a] C. Brückner, J. J. Posakong, R. W. Boyle, B. R. James, D. Dolphin, *J. Porphyrins Phthalocyanines* **1998**, *2*, 455–465. – [27b] J. S. Manka, D. S. Lawrence, *Tetrahedron Lett.* **1989**, *30*, 6989–6992.
- [24] Stable porphodimethenes were first described by Buchler: J. W. Buchler, L. W. Puppe, *Justus Liebigs Ann. Chem.* **1970**, *740*, 142–163. J. W. Buchler, L. W. Puppe, *Justus Liebigs Ann. Chem.* **1974**, 1046–1062. P. N. Dwyer, L. Puppe, J. W. Buchler, W. R. Scheidt, *Inorg. Chem.* **1975**, *14*, 1782–1785. J. W. Buchler, K. L. Lay, Y. L. Lee, W. R. Scheidt, *Angew. Chem.* **1982**, *94*, 457–457. A. Botulinski, J. W. Buchler, K.-L. Lay, H. Stoppa, *Liebigs Ann. Chem.* **1984**, *7*, 1259–1267. A. Botulinski, J. W. Buchler, N. E. Abbes, W. R. Scheidt, *Liebigs Ann. Chem.* **1987**, 305–309.
- [25] S. Runge, M. O. Senge, *Z. Naturforsch., Teil B* **1998**, *53*, 1021–1030. M. O. Senge, M. Speck, K. Ruhlandt-Senge, *Tetrahedron* **2000**, *56*, 8927–8932.
- [26] H. Ogoshi, H. Sugimoto, T. Nishiguchi, T. Watanabe, Y. Matsuda, Z. Yoshida, *Chem. Lett.* **1978**, *30*, 29–34.
- [27] K. M. Smith, D. A. Goff, D. J. Simpson, *J. Am. Chem. Soc.* **1985**, *107*, 4946–4954.
- [28] H. J. Callot, A. Louati, M. Gross, *Tetrahedron Lett.* **1980**, *21*, 3281–3284.
- [29] K. M. Zaman, S. Yamamoto, N. Nishimura, *J. Am. Chem. Soc.* **1994**, *116*, 12099–12100.
- [30] M. J. Crossley, L. G. King, J. L. Simpson, *J. Chem. Soc., Perkin Trans. 1* **1997**, 3087–3096.
- [31] A. B. J. Parusel, T. Wondimagegn, A. Ghosh, *J. Am. Chem. Soc.* **2000**, *122*, 6371–6374.
- [32] J. L. Hoard, *Science* **1971**, *174*, 1295–1301.
- [33] [33a] D. L. Cullen, E. F. Meyer Jr., *J. Am. Chem. Soc.* **1974**, *96*, 2095–2102. – [33b] E. F. Meyer Jr., *Acta Crystallogr., Sect. B* **1972**, *28*, 2162–2167.
- [34] J. W. Lauher, J. A. Ibers, *J. Am. Chem. Soc.* **1973**, *95*, 5148–5152.
- [35] A. Regev, T. Galili, C. J. Medforth, K. M. Smith, K. M. Barkigia, J. Fajer, H. Levanon, *J. Phys. Chem.* **1994**, *98*, 2550–2526.
- [36] The  $\Delta_{24}$  value gives the average deviation of the 24 macrocycle atoms from their least-squares-plane and is a measure of the overall out-of-plane distortion. The core size ( $\otimes$ ) is defined as the average length of the vectors connecting the pyrrole nitrogen atoms with the geometrical center of the 4N unit. It is a measure for the size of the central coordination hole. The core elongation parameter ( $\Xi$ ) is defined as the difference between the length of the vectors connecting the sides of the 4N unit:  $\Xi = |\text{N}21 \rightarrow \text{N}22 + \text{N}23 \rightarrow \text{N}24| - |\text{N}22 \rightarrow \text{N}23 + \text{N}24 \rightarrow \text{N}21|$ ; it is a measure for the in-plane distortion of the 4N core.
- [37] The solvate molecule is located on the more symmetric and better shielded, but less distorted face of the porphyrin overall. In orientation given for **14** in Figure 7 this is the lower part of the skeletal deviation plot.
- [38] [38a] J. L. Sessler, A. Mozattari, M. Johnson, *Org. Synth.* **1991**, *10*, 68–77. D. H. R. Barton, J. Kervagore, S. Zard, *Tetrahedron* **1990**, *46*, 7587–7593. J. B. Paine, W. B. Kirshner, D. W. Moskowitz, *J. Org. Chem.* **1976**, *41*, 3857–3859. – [38b] J. E. Falk, in: *Porphyrins and Metalloporphyrins*, Elsevier Publishing Company, Amsterdam, London, New York, **1965**, Vol. II, p.138.
- [39] Crystallographic data (excluding structure factors) for the structures reported in this paper have been deposited with the Cambridge Crystallographic Data Centre as supplementary publication no. CCDC-150529–150537. Copies of the data can be obtained free of charge on application to CCDC, 12 Union Road, Cambridge CB2 1EZ, UK [Fax: (internat.) + 44(1223)336-033; E-mail: deposit@ccdc.cam.ac.uk].
- [40] H. Hope, *Prog. Inorg. Chem.* **1994**, *41*, 1–19.
- [41] [41a] S. R. Parkin, B. Moezzi, H. Hope, *J. Appl. Crystallogr.* **1995**, *28*, 53–56. – [41b] G. M. Sheldrick, *SADABS*, Universität Göttingen, **1997**.
- [42] [42a] G. M. Sheldrick, *SHELXS-93*, Universität Göttingen, **1993**. – [42b] G. M. Sheldrick, *XL-97*, Universität Göttingen, **1997**.
- [43] H. D. Flack, *Acta Crystallogr., Sect. A* **1983**, *39*, 876–881.

Received October 6, 2000

[O00519]